UNIVERSITY OF CAMPINAS

SCHOOL OF MECHANICAL ENGINEERING

UNDERGRADUATION COMMISSION IN CONTROL AND AUTOMATION ENGINEERING

DEPARTMENT OF COMPUTATIONAL MECHANICS

UNDERGRADUATE THESIS

Cooperative Control of Dynamical Systems Based on a Time-Varying Lyapunov Function

Experimental Implementation in an Inverted Pendulum and an Active Suspension

Thesis Supervisor: Grace Silva Deaecto
Author: Arturo Moises Flores Alvarez

3.1415926 · · ·

Acknowledgements

I would like to give a warm and affectionate thanks to Moises, Aida, Crisaida and Francisco, my dear family. They have been a transcendental support during this university stage as well they have been for my life itself so. Thank you very much for all your love in these 22 years and for accompanying me in every decision I make.

I thank my supervisor, Grace Silva Deaecto, for giving me the opportunity to share a wonderful experience in the exciting world of research. Thank you very much for trusting me and choosing me to be part of your work and research team. I recognize and thank you infinitely for your patience, tact and dedication in the elaboration of this undergraduate thesis. Without your support, this work could not have came true.

I would like to give a special thanks to my alma mater, the National Engineering University, for having supported me academically, allowing me to meet wonderful and dazzling people, and also having supported me financially on projects that I have undertaken during my stay there. Without a doubt, I am very proud to have studied in that institution.

Finally, I would like to recognize all the friends who have supported me emotionally with some words of encouragement or with their time or with their piece of advice. Their good desires and good vibes have allowed me to take a break in this stressful university life. In that sense, I would like to mention Lucas and Helder for his good humor, patience and kindness to solve my doubts during the afternoons where I performed my experiments to do this thesis.

I put a momentary pause in this short list of thanks, to move on to describe to the reader my work in these months on a topic that I am very passionate about: Systems control.

Abstract

FLORES ALVAREZ, Arturo Moises. $\mathcal{H}_2$ *Cooperative Control of Dynamical Systems Based on a Time-Varying Lyapunov Function: Experimental Implementation in an Inverted Pendulum and an Active Suspension*, School of Mechanical Engineering, University of Campinas, 2019. Undergraduate thesis.

This undergraduate thesis treats the control design and practical implementation of a switched cooperative networked control of a set of linear time-invariant systems. The control design takes into account that the communication network presents limited bandwidth and that, at each instant of time, only one of the systems is allowed to receive the updated control signal, while the others must remain with the previously received controlled input. Hence, our main goal is to synthesize a cooperative resource sharing dynamic strategy assuring stability and an $\mathcal{H}_2$ guaranteed performance index. This strategy acts as a coordinator managing the control signal transmission among the systems and is mathematically represented by a switching rule that will choose at each decision interval, which system must receive the updated control law. The design conditions are based on a time-varying Lyapunov function and expressed in terms of Linear Matrix Inequalities (LMIs), being easy to solve by readily available tools. The control strategy has been experimental validated in the control of two mechanical systems, an inverted pendulum mounted on a motor-driven car that moves on a rail and an active suspension. The main idea is to synthesize the control effort to be transmitted cooperatively through the network to act in both systems in order to maintain the pendulum in the inverted vertical position, while attenuates the perturbations of the road profile in the active suspension. Initially, the mechanical system is analyzed, modeled and identified in a simple and precise manner. Afterward, the control technique is obtained and compared with the methodology based on Lyapunov-Metzler inequalities. Finally, experimental results and simulations show the efficiency of the proposed control technique.

Keywords: Cooperative control, switched systems, state-feedback control design, time-varying Lyapunov function, linear matrix inequalities.

List of Figures

List of Tables

Symbol List

I	-	Identity matrix.
$\mathbb{N}$	-	Set of natural numbers.
$\mathbb{Z}$	-	Set of integer numbers.
$\mathbb{R}$	-	Set of real numbers.
$\mathbb{R}^{m\times n}$	-	Set of real matrices of dimension $m \times n$
$\mathbb{K}$	-	Set of N positive natural numbers $\{1, \ldots, N\}$.
$F(s)$	-	Laplace transform of the function $f(t)$.
$F(z)$	-	$\mathcal{Z}$ transform of the function $f[k]$.
$\mathcal{L}\{f(t)\}$	-	Laplace transform operator applied to the function $f(t)$.
$\mathcal{Z}\{f[n]\}$	-	$\mathcal{Z}$ transform operator applied to the function $f[n]$.
$\|\xi\|_2^2$	-	Square norm of a trajectory $\|\xi\|_2^2 = \int_0^\infty \|\xi\|^2 dt$ ($\|\xi\|_2^2 = \sum_{n\in\mathbb{N}} \|\xi\|^2$) for the continuous(discrete)-time domain, where $\|\xi\|^2 = \xi'\xi$ is the Euclidean norm.
$\mathcal{L}_2$	-	Set of all the trajectories $\xi(t)$ ($\xi[n]$) in the continuous(discrete)-time domain such that $\|\xi\|_2 < \infty$.
A'	-	Transpose of the real matrix A.
$A(j\omega)^*$	-	Conjugate of the complex matrix $A(j\omega)$
$A(j\omega)^\sim$	-	Conjugate transpose of the complex matrix $A(j\omega)$
$P > 0$	-	Symmetric positive definite matrix P.
$P < 0$	-	Symmetric negative definite matrix P.
diag$\{A, B\}$	-	Diagonal block-matrix formed by the matrices A and B.
tr(A)	-	Trace of the matrix A.
Λ	-	Unit simplex defined as $\Lambda = \{\lambda \in \mathbb{R}^N \ : \ \lambda_i \geq 0, \ \sum_{i\in\mathbb{K}} \lambda_i = 1\}$.
A_λ	-	Convex combination of matrices $\{A_1, \cdots, A_N\}$, that is, $A_\lambda = \sum_{i\in\mathbb{K}} \lambda_i A_i$.
$a \bmod b$	-	Definition of the module operation which is the Euclidean division between the integers a and b.
$k(n)$	-	Definition of the $k(n) = n \mod \kappa$ for a given $\kappa \in \mathbb{N}$

Contents

Chapter 1

Introduction

Nowadays, the world is getting more connected. From a simple home network to the world wide spread internet, we appreciate that most of our daily actions involves create, send and receive data for multiple purposes. For example, the modern concept of Internet of Things is creating a necessity of the control in business, industrial and even domestic environments. As a result, networked control is allowing more users to create interaction among a finite number of of systems, in which signals from sensors, controllers and actuators are transmitted through shared network channels with the flexibility of information traffic between their components.

Therefore, during the control design, it is important to take into account physical limitations that may occur during transmission and are intrinsic of the communication network, such as bandwidth limitation, delay and quantization errors. These aspects, which are traditionally studied in communication theory, must be strongly considered in the control design for a proper performance and stability of the overall networked systems. An omission of these facts could lead our system to instability. The references (HESPANHA; NAGHSHTABRIZI; XU, 2007) and (WANG; LIU, 2008) provide theoretical background and introduce the reader to the main challenges to overcome over control through communication networks. Based on this, the study of systems with sampled-data has gained special importance because they allow to model the bandwidth limitation in a communication channel, see (SOUZA et al., 2014). The references (MAZO; TABUADA, 2008) and (MENG; CHEN, 2014) are also important because they present strategies of self-triggering and event-triggering as a solution to tackle the consumption of control signal transmission resources over the network.

On the other hand a topic of great current interest is the study of switched systems. They are defined by a finite number of subsystems and a switching rule. This rule can be arbitrary, playing the role of an external disturbance, or a control variable that, when is properly designed, can ensure stability and improve overall system performance. For this study, we will consider the case where the switching rule is a control variable to be designed. We recommend the reader to see the references (DECARLO et al., 2000), (HESPANHA; MORSE, 2002) and (SHORTEN et al., 2007) and the books (LIBERZON, 2013) and (SUN, 2006) that provide the theoretical basis of this important class of systems. In the network control context, the strategies based on commutation have been implemented in (DAI; LIN; GEE, 2009), (DONKERS et al., 2009) in order to prevent collision of information in the network channel. Figure (1.1) presents the control architecture scheme to be adopted in this study. As it can be seen, the plants receive the control signal that is transmitted by the network.

In order to avoid data packet loss, which is quite common when there is information going through a network, we assume that at each time interval the control signal is sent to only one of the plants and occupies the communication channel. Therefore, only this plant receives the updated

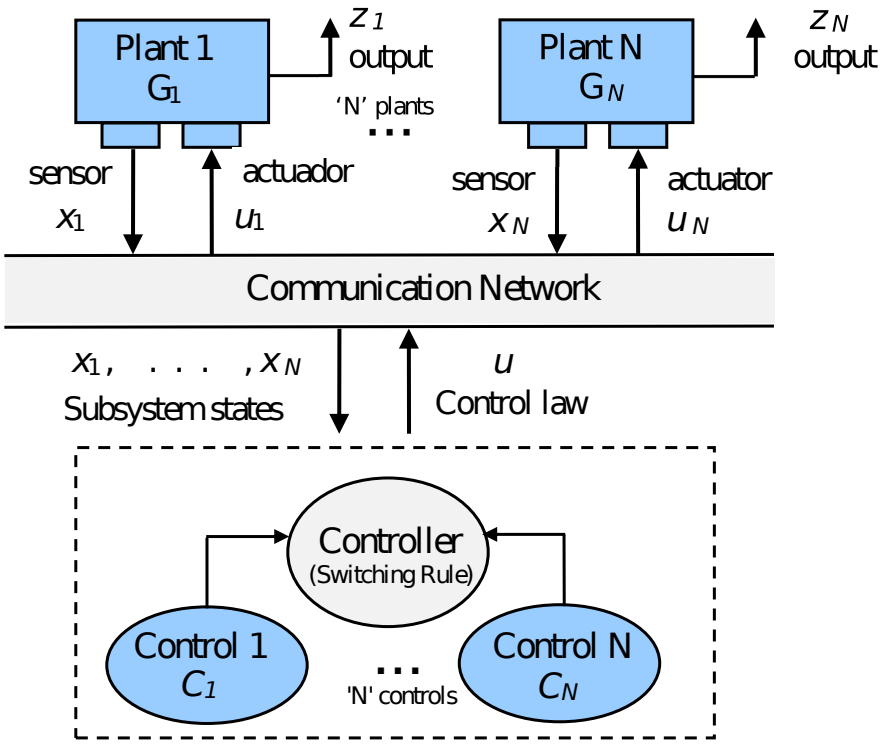

Figure 1.1: Control Architecture

control signal, while the others maintain the previous control law. Notice that the control law of all plants must remain constant over a period of time, chosen in order to respect the communication channel bandwidth. The choice of which plant receives the updated information is made by a coordinator, represented mathematically by the switching rule. Global control is responsible for ensuring stability and a guaranteed cost of performance. In this thesis, our aim is to treat the joint design of state-feedback feedback gains, important to synthesize the control law $u(\cdot)$, and the logic of the coordinator $\sigma(\cdot)$ by means of a time-varying Lyapunov function in order to ensure overall system stability and suitable $\mathcal{H}_2$ performance.

The theory is experimentally validated through the cooperative control of an inverted pendulum mounted on a motor-driven car that moves on a trail and an active suspension, both from the Quanser®company, see (QUANSER, 2012b) and (QUANSER, 2012a). The inverted pendulum has an interesting characteristic that can be clearly observed, for example, in the dicycle segway , which is a brand-new transport system widely used today for tourism and safety schemes around world. Additionally, the active suspension is important in automotive industries, where one of the main interest is to design novel control techniques for the suspension in order to isolate the vehicle chassis from road profile perturbations, maintaining the vehicle stable in irregular surfaces and promoting a good level of comfort for the passengers. Studies related to cooperative control can be seen in (LUZ NETTO, 2018), (SOUSA; GEROMEL; DEAECTO, 2015) but taking into account conditions based on Lyapunov-Metzler inequalities, which are nonconvex and, therefore, very difficult to solve for an arbitrary number of systems. Our contribution in this thesis is to provide alternative conditions, but expressed in terms of Linear Matrix Inequalities (LMIs), which are simpler and can be solved without difficulty by readily available tools. It is important to highlight that although simpler, the conditions are not more conservative than the ones based on Lyapunov-Metzler inequalities.

1.1 Summary description of the chapters

This dissertation is divided into five chapters, which are summarized below:

- **Chapter 1: Introduction.** In this chapter, we introduce the problem to be addressed in this thesis. Emphasizing its importance, specially in the context of network control, which together with the 'Internet of Things', make up one of the most important subjects currently being studied by the scientific community of control and computing.

- **Chapter 2: Fundamental Concepts.** This chapter presents a review of fundamental concepts related to dynamical systems. Initially, we present the Lyapunov stability criterion and the calculation of $\mathcal{H}_2$ norm for linear and time-invariant systems. Subsequently, we discuss about topics related to switched systems, as they will be widely used to obtain our main results. An academical example illustrates important concepts on the control technique to be adopted in this thesis.

- **Chapter 3: Modelling and Identification.** In this chapter, we perform a technical modelling of the inverted pendulum as well as the identification of its parameters. We will make special emphasis in the parameters that may vary due to external factors such as wear deterioration. We present also the model of the active suspension, but in this case we have considered the parameters provided by the manufacturer. At the end of the chapter, we discuss the models and their validation that will be used in the next chapter for the control design.

- **Chapter 4: Cooperative Control.** In this chapter, we present our main results. More specifically, we develop the cooperative control design conditions based on a time-varying Lyapunov function and compare the results with the ones derived from Lyapunov-Metzler inequalities. Additionally, we validate experimentally the theory in the cooperative control of the pendulum and the suspension showing its efficacy and accuracy.

- **Chapter 5: Conclusions and Perspectives for Future Researches.** Finally, this chapter draws the main conclusions and provides some interesting topics for future investigation.

Chapter 2

Fundamental Concepts

The aim of this chapter is to introduce some fundamental concepts well established in the literature that are the basis for the study of dynamical systems. First, we will present the linear time invariant system to be considered for stability and performance analysis. Then, the Lyapunov stability criterion is provided together with the definition and the calculus of the $\mathcal{H}_2$ norm by observability gramian and linear matrix inequalities (LMIs). Finally, we will introduce some important concepts related to switched linear systems, since they are one of the main focus of this undergraduate thesis.

2.1 Linear time invariant systems

Consider a linear time invariant system (LTI) described by the following state space representation

$$\begin{aligned} \dot{x}(t) &= Ax(t) + Hw(t),\ x(0) = 0 \\ z(t) &= Cx(t) + Ew(t) \end{aligned} \tag{2.1}$$

where $x(t) \in \mathbb{R}^{n_x}$ is the state vector, $w(t) \in \mathbb{R}^{n_w}$ is the external input and $z(t) \in \mathbb{R}^{n_z}$ is the controlled output. The transfer function $H_{wz}(s) \in \mathbb{C}^{n_z \times n_w}$ between the external input $w(t)$ and the controlled output $z(t)$ is

$$H_{wz}(s) = C(sI - A)^{-1}H + E \tag{2.2}$$

This system is classified as strictly proper when $E = 0$ or proper otherwise. Next, we discuss important classical concepts concerning the stability and performance of this system.

2.2 Stability

In this section, we present the Lyapunov stability criterion for LTI systems. This criterion is one of the most used and can be found in almost all the bibliography of control theory, such as (GEROMEL; KOROGUI, 2001), (KHALIL, 2002), (SLOTINE; LI, 1991). First, let us consider a simpler LTI system:

$$\dot{x}(t) = Ax(t),\ x(0) = x_0 \tag{2.3}$$

where whenever matrix A is nonsingular, the origin $x_e = 0$ is its unique equilibrium point. This point is defined as the one such that $x(t_0) = x_e$ for some $t = t_0$, then $x(t) = x_e$ for all $t \geq t_0 \geq 0$. Considering a function $V(x)$ that measures the distance between a generic point x and the equilibrium x_e, if for all initial condition $x(0) = x_0$ the function $V(x(t))$ decreases and tends to zero through the time, then the point x_e is said to be globally asymptotically stable. The

Lyapunov criterion is based on the choice of this function and in the imposition that it be always decreasing with respect to the time $t \geq 0$. Then, choosing the following quadratic Lyapunov function candidate

$$V(t) = x'Px, \tag{2.4}$$

where $P > 0$, we have that its time derivative evaluated for an arbitrary solution of (2.3) is given by

$$\begin{aligned} \frac{dV(x(t))}{dt} &= \dot{V}(t) \\ &= \dot{x}'Px(t) + x^T P\dot{x} \\ &= x'(A'P + PA)x \end{aligned} \tag{2.5}$$

Notice that, the function $V(x)$ is positive definite for all $x \neq x_e$ whenever matrix P is positive definite. Analogously, its time derivative $\dot{V}(x)$ is negative definite for all $x \neq x_e$, whenever following condition

$$A'P + PA = -Q < 0 \tag{2.6}$$

is verified for an arbitrary positive definite matrix $Q > 0$ given. In this case, we can say that the equilibrium point $x_e = 0$ is globally asymptotically stable. The next lemma presents the Lyapunov stability criterion specific for LTI systems.

Lemma 2.1 *(GEROMEL; KOROGUI, 2001) The LTI system (2.3) is globally asymptotically stable if and only if, for a given matrix $Q > 0$, there exists a matrix $P > 0$ that is the unique solution of the Lyapunov equation $A^T P + PA + Q = 0$.*

In this lemma, the sufficiency follows from (2.6), which indicates that whenever its is verified then $\dot{V}(x) < 0$ and the system is globally asymptotically stable. Now let us show the necessity. Indeed, supposing that the system is globally asymptotically stable let us show that matrix

$$P = \int_0^\infty e^{A't} Q e^{At} dt \tag{2.7}$$

is the unique positive definite solution of the Lyapunov equation. Indeed, multiplying (2.7) from the right by ξ and from the left by its transpose, we obtain

$$\xi' P \xi = \int_0^\infty \xi' e^{A't} Q e^{At} \xi dt = \int_0^\infty x' Q x dt \tag{2.8}$$

where $x = e^{At}\xi$ is the solution of the system $\dot{x} = Ax$ for the initial condition $x(0) = \xi$. As $Q > 0$ then $\xi' P \xi > 0$. Furthermore, it satisfies the Lyapunov equation, as follows:

$$\begin{aligned} A'P + PA &= \int_0^\infty \frac{d}{dt}\left(e^{A't} Q e^{At}\right) dt \\ &= \lim_{t\to\infty} e^{A't} Q e^{At} - Q = -Q \end{aligned} \tag{2.9}$$

where the third equality is due to the fact that the indicated limit is null, since by hypothesis the system is globally asymptotically stable. In the next section, we will introduce the definition of $\mathcal{H}_2$ norm of a dynamical system, which will be very useful for the forthcoming developments.

2.3 $\mathcal{H}_2$ Norm

In this section, we present the $\mathcal{H}_2$ norm, which is one of the performance criteria more used for measuring the quality of the control design in dynamical systems (GEROMEL; KOROGUI, 2001). For this purpose let us consider the more general system defined in the beginning of this chapter and given by (2.1). This norm is defined for strictly proper transfer functions that are asymptotically stable, but can also be determined from their impulsive responses. This is possible due to the Parseval's Theorem, that allows us to obtain a direct relation between the time domain and the frequency domain, see (GEROMEL; KOROGUI, 2001) for details.

Theorem 2.1 ***(Parseval's Theorem)*** *Consider a real function* $f(t) : \mathbb{R}^+ \to \mathbb{R}$ *such that* $F(s) = \mathcal{L}\{f(t)\} : \mathcal{D}\{F(s)\} \to \mathbb{C}$ *with* $0 \in \mathcal{D}\{F(s)\}$*, so the following equality is verified:*

$$\int_0^\infty f(t)^2 dt = \frac{1}{\pi}\int_0^\infty F(j\omega)^* F(j\omega) d\omega \tag{2.10}$$

Proof: In fact, equality (2.10) is based on the inverse Laplace transform of $f(t)$ with $s = j\omega$, that is

$$f(t) = \frac{1}{2\pi j}\int_\Gamma F(s)e^{st}dt = \frac{1}{2\pi}\int_{-\infty}^{+\infty} F(j\omega)e^{j\omega t}d\omega \tag{2.11}$$

where Γ is the imaginary axis that belongs to the domain of $F(s)$. Taking the definition of $\mathcal{L}_2$ norm, we obtain:

$$\begin{aligned}
\|f(t)\|_2^2 &= \int_0^\infty f(t)^2 dt \\
&= \int_0^\infty f(t)\Big(\frac{1}{2\pi}\int_{-\infty}^{+\infty} F(j\omega)e^{j\omega t}d\omega\Big)dt \\
&= \frac{1}{2\pi}\int_{-\infty}^{+\infty}\Big(\int_0^\infty f(t)e^{-j\omega t}dt\Big)^* F(j\omega)d\omega \\
&= \frac{1}{2\pi}\int_{-\infty}^{+\infty} F(j\omega)^* F(j\omega)d\omega dt
\end{aligned} \tag{2.12}$$

Moreover, as $f(t)$ is a real function, then $F(j\omega) = F(-j\omega)$ and thus:

$$\|f(t)\|_2^2 = \frac{1}{2\pi}\int_{-\infty}^{\infty} F(j\omega)^* F(j\omega)d\omega = \frac{1}{\pi}\int_0^\infty F(j\omega)^* F(j\omega)d\omega \tag{2.13}$$

as provided in (2.10). □

The $\mathcal{H}_2$ norm for an LTI system can be computed for a transfer function $H_{wz}(s)$, strictly proper, analytic in the complex right half-plane including the imaginary axis and it is defined as follows:

$$\|H_{wz}(s)\|_2 = \left(\frac{1}{2\pi}\int_{-\infty}^{\infty}\mathrm{Tr}(H_{wz}(j\omega)^\sim H_{wz}(j\omega))d\omega\right)^{1/2} \tag{2.14}$$

Using the Parseval's theorem we can determine this norm alternatively by

$$\|H_{wz}(s)\|_2^2 = \int_0^\infty \mathrm{Tr}(h_{wz}(t)' h_{wz}(t)dt \tag{2.15}$$

where $h_{wz}(t) = Ce^{At}H + E\delta(t)$ is the impulsive response of (2.1). Taking this impulsive response, we obtain:

$$\begin{aligned}\|H_{wz}(s)\|_2^2 &= \int_0^\infty \mathrm{Tr}\Big((Ce^{At}H + E\delta(t))'(Ce^{At}H + E\delta(t))\Big)dt \\ &= \mathrm{Tr}\Big(H'\Big(\int_0^\infty e^{A't}C'Ce^{At}dt\Big)H\Big) + 2\mathrm{Tr}(H'C'E) \\ &+ \mathrm{Tr}(E'E)\int_0^\infty \delta(t)^2 dt\end{aligned} \tag{2.16}$$

Notice that this norm is finite only if the system is strictly proper, since we have

$$\int_0^\infty \delta(t)^2 dt = \frac{1}{\pi}\int_0^\infty d\omega \to \infty \tag{2.17}$$

which makes imperative to impose that $E = 0$.

Therefore, for strictly proper systems, the $\mathcal{H}_2$ norm is defined as follows:

$$\|H_{wz}(s)\|_2^2 = \{\mathrm{Tr}(H'P_oH) \ : \ A'P_o + P_oA + C'C = 0\} \tag{2.18}$$

where

$$P_o = \int_0^\infty e^{A't}C'Ce^{At}dt \tag{2.19}$$

is the observability Gramian.

Alternatively, this quantity can be computed as a solution of the following convex optimization problem.

$$\|H_{wz}(s)\|_2^2 = \inf_{P>0}\{\mathrm{Tr}(H'PH) \ : \ A'P + PA + C'C < 0\} \tag{2.20}$$

In fact, note that each solution $P > 0$ of the inequality:

$$A'P + PA + C'C < 0 \tag{2.21}$$

satisfies the Lyapunov 's equation $A'P + PA + C'C = -S$ for an arbitrary matrix $S > 0$. Then, we obtain

$$P = \int_0^\infty e^{A't}(C'C + S)e^{At}dt > P_o \tag{2.22}$$

and, therefore, with the infimum presented in (2.20) the solution P approaches arbitrarily of P_o. The problem (2.20) is described in terms of LMIs (see (BOYD et al., 1994)) and can be solved without difficulty by the algorithms available in the literature. Moreover, this description is more amenable for output and state feedback control generalizations. The next section presents some important features of switched systems, which will be our focus throughout this study.

2.4 Switched systems

A switched system is a dynamical system that is formed by a finite number of subsystems and a switching function that selects a subsystem at each instant of time in order to assure stability and improve performance. Some references that discuss about this theme are (FIACCHINI; JUNGERS, 2014), (FIACCHINI; GIRARD; JUNGERS, 2016), (GEROMEL; COLANERI, 2006a). The interest in such kind of systems relies in their capability of modeling complex real systems, as embedded or networked ones, and also for the theoretical issues involved. In fact, their dynamical properties are often not intuitive nor trivial. As for instance, a switched system presents intrinsic dynamics that occur when it evolves on a sliding mode and that do not coincide with the one of any of the subsystems, see (LIBERZON, 2013). In this sense, a suitable switching function can assure stability even if all subsystems are unstable (GEROMEL; DEAECTO; DAAFOUZ, 2013).

There exist two important classes of switching functions, which have attracted the attention of the scientific community in the last decades. In the first, the switching rule is arbitrary and the goal is to determine the minimum dwell time, that is, a minimum period of time in which the commutation is not allowed, in order to preserve stability and improve performance. In the second class, it is a control variable $\sigma(x(t)) : \mathbb{R}^{n_x} \to \{1, 2, \ldots, N\} := \mathbb{K}$ to be designed in order to accomplish the same goals.

In this thesis we focus on the second group of switching functions. More specifically, our goal is to obtain sufficient conditions for the control design of a switching function for discrete-time switched linear systems taking into account an $\mathcal{H}_2$ performance criterion to be defined afterwards. In this sense, this chapter presents some important results, already available in the literature, that are specific for this class of systems. Basically, we will provide Lyapunov-Metzler conditions based on a min-type Lyapunov function obtained from (GEROMEL; COLANERI, 2006b) and LMI conditions based on a time-varying Lyapunov function available in (DEAECTO; GEROMEL, 2018). These last conditions will be generalized in Chapter 4 to cope with cooperative control design.

2.4.1 Problem statement

Consider the following switching system defined $\forall\, n \in \mathbb{N}_-$ where $\mathbb{N}_- = \mathbb{N} \cup \{-1\}$

$$\begin{aligned} x[n+1] &= A_\sigma x[n] + H_\sigma w[n],\ x[-1] = 0 \\ z[n] &= C_\sigma x[n] \end{aligned} \tag{2.23}$$

where $x \in \mathbb{R}^{n_x}$, $w \in \mathbb{R}^{n_w}$, $z \in \mathbb{R}^s$ are the state, the exogenous input and the controlled output, respectively. Moreover $w(n) = \delta(n+1)e_r$ is the impulsive response and e_r is the standard basis. First, note that this system is equivalent to

$$\begin{aligned} x[n+1] &= A_\sigma x[n],\ x(0) = H_{\sigma[-1]} e_r \\ z[n] &= C_\sigma x[n] \end{aligned} \tag{2.24}$$

defined for all $n \in \mathbb{N}$. This alternative description is usual in the literature, whenever the $\mathcal{H}_2$ performance index is taken into account, see (GEROMEL; COLANERI; BOLZERN, 2008) for details.

For the system in (2.23) the control action is accomplished by means of a switching function $\sigma(x) : \mathbb{R}^{n_x} \to \mathbb{K}$ to be designed. For a given performance index $J(\sigma)$, the main objective is to determine an optimal switching function that minimizes the following criterion

$$\inf_{\sigma \in \mathbb{V}} J(\sigma) \tag{2.25}$$

where $\mathbb{V}$ is the set of all globally asymptotically stable switching functions. This problem is very difficult to solve due to the nonlinear nature of the switching function. Hence, the idea is to assure a suitable upper bound for (2.25) and to obtain a suboptimal solution. At this point, it is necessary to define the performance index to be considered in this thesis.

Definition 2.1 *The $\mathcal{H}_2$ performance index associated with the closed-loop switched linear system (2.23) with initial condition $x[-1] = 0$ is given by*

$$J_2(\sigma) = \sum_{r=1}^{n_w} \|z_r\|_2^2 \tag{2.26}$$

where z_r is the controlled output corresponding to the impulsive input $w[n] = e_r\delta[n+1]$, for all $r = 1, ..., n_w$.

The next subsection presents conditions for the control design of the switching function assuring an upper bound for the $\mathcal{H}_2$ performance index (2.26).

2.4.2 Stability and $\mathcal{H}_2$ performance

Let us first consider the min-type Lyapunov function given by

$$V(x) = \min_{i\in\mathbb{K}} x'P_i x \tag{2.27}$$

where $P_i > 0,\ \forall i \in \mathbb{K}$, as well as the associated switching function

$$\sigma(x) = \arg\min_{i\in\mathbb{K}} x'P_i x \tag{2.28}$$

Notice that, (2.27) is nonconvex and non-differentiable at the points where the minimum operator occurs for more than one index. Define the subclass of Metzler matrices $\Pi \in \mathcal{M}$ composed by all matrices $\Pi \in \mathbb{R}^{N\times N}$ such that

$$\pi_{ij} \geq 0,\ (i,j) \in \mathbb{K}\times\mathbb{K}, \quad \sum_{i\in\mathbb{K}} \pi_{ji} = 1, \tag{2.29}$$

since it will be important for the forthcoming results. The next theorem, borrowed from reference (GEROMEL; COLANERI, 2006b) presents the stability conditions for (2.23).

Theorem 2.2 *Assume that there exist matrices $P_i > 0$ and a Metzler matrix $\Pi \in \mathcal{M}$ satisfying the following Lyapunov-Metzler inequalities*

$$A_i' \left(\sum_{j\in\mathbb{K}} \pi_{ji}P_j\right) A_i - P_i + C_i'C_i < 0,\ i \in \mathbb{K} \tag{2.30}$$

Then, the state-dependent switching function (2.28) assures the global asymptotic stability of the system (2.23) and satisfies

$$J_2(\sigma) < \min_{i\in\mathbb{K}} \mathrm{Tr}(H_m'P_iH_m) \tag{2.31}$$

for a given $m = \sigma[-1]$.

Proof: The proof is available in (GEROMEL; COLANERI; BOLZERN, 2008) and for this reason will be omitted. □

About this result, some remarks are in order. The first one is that a necessary condition for the feasibility of (2.30) is the validity of the following inequalities

$$(\sqrt{\pi_{ii}}A_i)' P_i (\sqrt{\pi_{ii}}A_i) - P_i < 0, \ i \in \mathbb{K} \tag{2.32}$$

which have been obtained by making $\sum_{j\in\mathbb{K}} \pi_{ji}P_j = \pi_{ii}P_i + \sum_{j\neq i\in\mathbb{K}} \pi_{ji}P_j$ in (2.30). Note that from the definition of the subclass of Metzler matrices present in (2.29), we have that $0 \leq \pi_{ii} \leq 1, \ \forall i \in \mathbb{K}$, and, therefore, matrices $\sqrt{\pi_{ii}}A_i$ must be stable as a necessary condition. Hence, it is not required any stability property of the matrices A_i considered separately. The second remark regards the computational solution of the Lyapunov-Metzler inequalities (2.30). These inequalities are nonconvex due to the product of matrix variables $\{\Pi, P_i, \ \forall i \in \mathbb{K}\}$ and, therefore, extremely difficult to solve for more than three subsystems. However, a simpler condition can be obtained by taking into account Metzler matrices with equal elements in the main diagonal, as proposed in (GEROMEL; COLANERI, 2006b). Although, simpler this alternative condition can be very conservative.

In order to circumvent this difficulty in the solution of the Lyapunov-Metzler inequalities, the literature has presented other control proposals, some of them based on LMIs as in the references (FIACCHINI; GIRARD; JUNGERS, 2016), (DEAECTO; GEROMEL, 2018). The idea is to provide alternative conditions that are simpler, but not more conservative than the ones presented in Theorem 2.2. In this direction, let us provide in the next developments the main results of (DEAECTO; GEROMEL, 2018), since they will be generalized to cope with cooperative control.

Before proceeding, it is important to make clear that the conditions to be obtained afterwards are based on a periodic time-varying Lyapunov-function defined as

$$V(x, n) = x'P[n]x \tag{2.33}$$

where $P[n] = P[k(n)]$ for all $n \in \mathbb{N}$. Notice that, this function presents period κ and that $P[0] = P[\kappa]$. Let us define the unit simplex Λ as being

$$\Lambda = \left\{ \lambda \in \mathbb{R}^N \ : \ \lambda_i \geq 0, \sum_{i\in\mathbb{K}} \lambda_i = 1 \right\} \tag{2.34}$$

that will be important in the next theorem, which presents the stability results and the $\mathcal{H}_2$ guaranteed cost for this case.

Theorem 2.3 *For a given positive scalar $1 \leq \kappa \in \mathbb{N}$, assume that there exist vectors $\lambda[n] \in \Lambda$ and matrices $P[n] > 0$ satisfying the inequalities*

$$\sum_{i\in\mathbb{K}} \lambda_i[n](A_i'P[n+1]A_i - P[n] + C_i'C_i) < 0 \tag{2.35}$$

for all $n = 0, \cdots, \kappa - 1$ with the boundary conditions $P[0] = P[\kappa]$. Then the state-dependent switching function

$$\sigma(x[n]) = \arg\min_{i\in\mathbb{K}} x[n]'(A_i'P[k(n)+1]A_i + C_i'C_i)x[n] \tag{2.36}$$

assures global asymptotic stability of the system (2.21) and satisfies

$$J_2(\sigma) < \mathrm{Tr}(H_m'P[0]H_m) \tag{2.37}$$

for a given $m = \sigma[-1]$.

Proof: The proof is available in (DEAECTO; GEROMEL, 2018), which assures exponential stability of the system (2.21). However, due to the importance of this theorem for the Chapter 4, its proof will be provided here, in a slightly different manner in order to assure asymptotic stability. Define the difference operator as being $\Delta V(x,n) = V(x,n+1) - V(x,n)$ and take into account the system (2.23) written alternatively as (2.24). Then, for an arbitrary trajectory of (2.24) defined for $n = 0, \cdots, \kappa - 1$, we have

$$\begin{aligned}
\Delta V(x,n) &= x[n+1]'P[n+1]x[n+1] - x[n]'P[n]x[n] \\
&= x[n]'(A_\sigma' P[n+1] A_\sigma - P[n] + C_\sigma' C_\sigma)x[n] - z[n]'z[n] \\
&= \min_{i \in \mathbb{K}} x[n]'(A_i' P[n+1] A_i - P[n] + C_i' C_i)x[n] - z[n]'z[n] \\
&= \min_{\lambda \in \Lambda} x[n]' \left(\sum_{i \in \mathbb{K}} \lambda_i[n] \Big(A_i' P[n+1] A_i - P[n] + C_i' C_i \Big) \right) x[n] - z[n]'z[n] \\
&\leq x[n]' \left(\sum_{i \in \mathbb{K}} \lambda_i[n] \Big(A_i' P[n+1] A_i - P[n] + C_i' C_i \Big) \right) x[n] - z[n]'z[n] \\
&< -z[n]'z[n]
\end{aligned} \tag{2.38}$$

where the third equality comes from the switching function (2.36), the fourth is due to a known property of the minimum operator and the last inequality follows from the validity of (2.35). From the periodic continuation $P[n] = P[k(n)]$, we have that inequality (2.35) holds for all $n \in \mathbb{N}$. Now, summing both sides of $\Delta V(x,n) < -z[n]'z[n]$ from $n = 0$ until infinity, we have that

$$\|z\|_2^2 < V(x,0) = x[0]'P[0]x[0] \tag{2.39}$$

since $\lim_{n\to\infty} V(x,n) = 0$ because the system is asymptotically stable. Remembering that $x[0] = H_m e_r$ and from definition (2.1), we have

$$\begin{aligned}
J_2(\sigma) &= \sum_{r=1}^{n_w} \|z_r\|_2^2 \\
&< \sum_{r=1}^{n_w} e_r' H_m' P[0] H_m e_r \\
&= \mathrm{Tr}(H_m' P[0] H_m)
\end{aligned} \tag{2.40}$$

completing thus the proof. □

Notice that the condition of Theorem 2.3 is nonconvex due to the product of variables $(\lambda[n], P[n])$ and, therefore, is extremely difficult to solve. Fortunately, a simplification can be adopted without loss of generally searching $\lambda[n]$ only on the vertices of the simplex $\lambda \in \Lambda_v \subset \Lambda$. This will allow us to describe the conditions (2.35) in terms of LMIs. Before continuing, some definitions are important. Let us denote the set $\mathfrak{C}(\kappa) = \mathbb{K}^\kappa$ which contains N^κ elements. The ℓ-th element is denoted by $\mathfrak{C}_\ell(\kappa) \in \mathfrak{C}(\kappa)$ where $1 \leq \ell \leq N^\kappa$. Moreover, each element $\mathfrak{C}_\ell(\kappa)$ contains κ terms in which $i[n] \in \mathfrak{C}_\ell(\kappa)$ for $n = 0, \cdots, \kappa - 1$. The next corollary provides a representation of Theorem 2.3 described in terms of LMIs.

Corollary 2.1 *For a given positive scalar $1 \leq \kappa \in \mathbb{N}$, assume that there exist matrices $P[n] > 0$ solution of the following optimization problem*

$$\min_{1 \leq \ell \leq N^k} \inf_{P[n] > 0} \mathrm{Tr}(H_m' P[0] H_m) \tag{2.41}$$

subject to

$$A'_{i[n]}P[n+1]A_{i[n]} - P[n] + C'_{i[n]}C_{i[n]} < 0 \tag{2.42}$$

for all $n = 0, \cdots, \kappa - 1$, $i[n] \in \mathfrak{C}_\ell(\kappa)$ *with the boundary conditions* $P[0] = P[\kappa]$. *Then, the state-dependent switching function (2.36) assures global asymptotic stability of the system (2.21) and satisfies (2.37) for a given* $m = \sigma[-1]$.

Proof: The proof follows directly from the fact that we can, without loss of generality, constraint the set of $\lambda[n] \in \Lambda$ to the ones belonging to the vertices, that is, $\lambda[n] \in \Lambda_v$, see reference (DEAECTO; GEROMEL, 2018) for more details about this proof. □

Compared to the Lyapunov-Metzler inequalities of Theorem 2.2, the conditions of Corollary 2.1 are much simpler to solve, since they are described in terms of LMIs. Moreover, as it has been discussed in (DAIHA et al., 2017), both conditions can not be compared in terms of conservatism. Indeed, both are a particular case of the time-varying Lyapunov-Metzler inequalities presented in (DAIHA et al., 2017) which although more general are impossible to solve because, besides the fact that they are nonconvex, they are also time-varying. The conditions of Theorem 2.2 is obtained eliminating the time-varying nature of the conditions provided in (DAIHA et al., 2017), while the conditions of Corollary 2.1 is obtained by imposing time-varying Metzler matrices with the same columns $\Pi[n] = [\lambda[n] \ \cdots \ \lambda[n]]$. Hence, for some cases Theorem 2.2 can be the best choice due to the generality of $\pi \in \mathcal{M}$ and in other cases the conditions (4.25) can provide better results due to its time-varying nature. In the next subsection, it is presented an illustrative example to compare both Theorem 2.2 and Corollary 2.1 and show the efficiency of the LMIs (2.42).

2.4.3 Example

Consider the system (2.23) composed of two unstable subsystems defined by $A_i = e^{A_{ci}h}, i \in \{1, 2\}$ with $h = 0.1$ [s] and the following matrices

$$A_{c1} = \begin{bmatrix} 0 & 1 & 0 \\ 0 & 0 & 1 \\ -45 & -29 & 1 \end{bmatrix}, \ H_1 = \begin{bmatrix} -1 \\ 1 \\ 1 \end{bmatrix}, \ C_1 = \begin{bmatrix} 3 & 0 & 2 \end{bmatrix} \tag{2.43}$$

$$A_{c2} = \begin{bmatrix} 0 & 1 & 0 \\ 0 & 0 & 1 \\ 10 & -5 & -50 \end{bmatrix}, \ H_2 = \begin{bmatrix} -1 \\ 1 \\ 1 \end{bmatrix}, \ C_2 = \begin{bmatrix} 1 & 0 & 2 \end{bmatrix} \tag{2.44}$$

We have solved the conditions of Theorem 2.2 by searching the parameters of the Metzler matrix inside a box $[0, 1] \times [0, 1]$ with step 0.1. We have obtained for the Metzler matrix

$$\Pi = \begin{bmatrix} 0 & 1 \\ 1 & 0 \end{bmatrix} \tag{2.45}$$

a guaranteed cost $J_2(\sigma) < J_{2s} = 129.91$ and the positive definite matrices

$$P_1 = \begin{bmatrix} 210.3146 & 130.9615 & -2.1225 \\ 130.9615 & 201.4047 & 14.5241 \\ -2.1225 & 14.5241 & 33.7353 \end{bmatrix}, \ P_2 = \begin{bmatrix} 216.4268 & 156.8974 & 5.0755 \\ 156.8974 & 224.3637 & 4.4851 \\ 5.0755 & 4.4851 & 4.0918 \end{bmatrix} \tag{2.46}$$

that are important for the switching function implementation. Afterwards, we have solved the LMI conditions of Corollary 2.1 for different values of $\kappa \in \{2, 3, 4, 5, 6\}$ obtaining the guaranteed

κ	J_{2s} - Cor. 2.1	$\sigma_P[n]$	$\sigma(x[n])$	J_{2s} - Theo. 2.2
2	129.9	129.9	86.009	
3	137.21	137.21	89.179	
4	129.9	129.9	96.331	129.91
5	127.691	127.69	95.513	
6	**124.96**	124.96	106.52	

Table 2.1: Performance indexes for different cases.

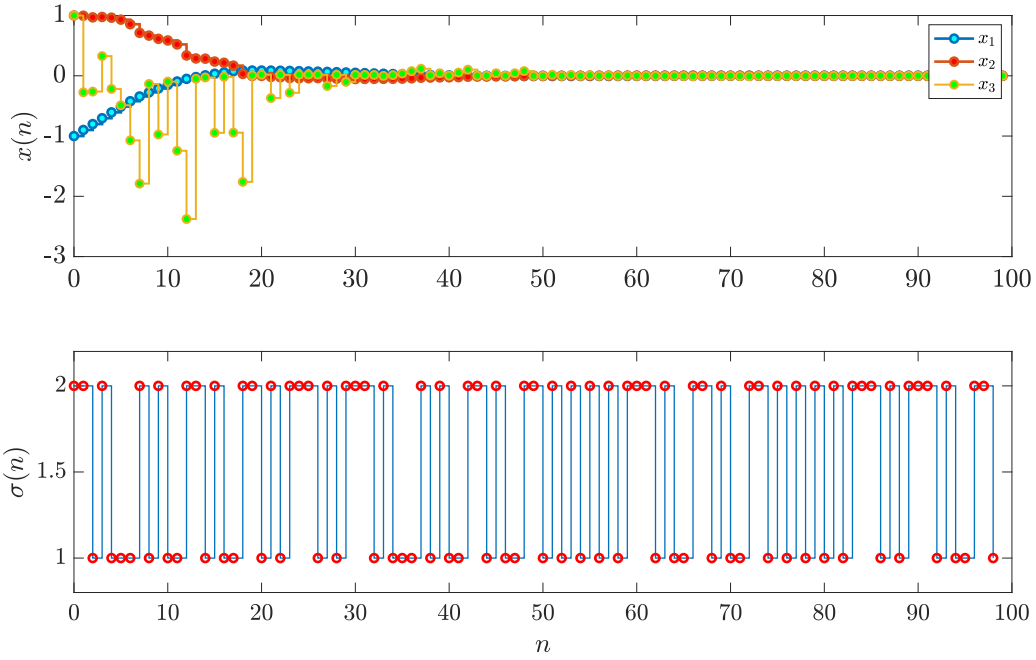

Figure 2.1: State trajectories and switching function.

costs J_{2s} presented in the second column of Table 2.1. For each κ we have implemented the periodic switching function $\sigma_P[n]$, obtaining the actual costs presented in the third column of the table. Notice that, these costs coincide with the guaranteed ones, indicating as discussed in (DEAECTO; GEROMEL, 2018) that the conditions of Corollary 2.1 are necessary and sufficient for the periodic switching function. We have also implemented the state-dependent switching function proposed in (2.36) obtaining the actual costs provided in the fourth column of Table 2.1. Notice that, this switching function has always enhanced the actual performance when compared with the periodic case indicating the efficiency of the adopted control technique.

Notice that the best guaranteed performance $J_{2s} = 124.96$ has been obtained for $\kappa = 6$, associated to the optimal sequence $\mathfrak{C}_{53}(6) = (2\ \ 2\ \ 1\ \ 2\ \ 1\ \ 1)$, and is smaller than the guaranteed cost obtained from the Lyapunov-Metzler inequalities. Figure 2.1 presents the state trajectories and the correspondent switching function obtained from the solution of Corollary 2.1 with $\kappa = 6$.

2.5 Final considerations

In this chapter, we have presented a series of fundamental concepts for analysis and control design of dynamic systems. Moreover, two recent results related to switched systems have been presented that will be very useful in the next chapters to address the cooperative control of several systems that share the same communication channel, which is the main subject of this thesis. More specifically, the concepts of stability and $\mathcal{H}_2$ norm were introduced for LTI systems, and after generalized to cope with switched systems. Regarding this class of systems, we have presented control design conditions borrowed from two very recent references (GEROMEL; COLANERI; BOLZERN, 2008) and (DEAECTO; GEROMEL, 2018). We have discussed and compared by means of an academical example the main features of both methodologies.

Chapter 3

Modeling and Identification

In this chapter, our main objective is to present the models of the two plants that will be used in Chapter 4 for the experimental validation of the cooperative control technique to be developed in the same chapter. The plants consist in an inverted pendulum coupled to a motor-driven car that moves on a rail and in an active suspension, both from Quanser company. The first plant is clearly nonlinear, which demands us to obtain a very precise model. Therefore, some physical parameters, as for instance, motor efficiency, viscous friction, among others, will be identified, since they can suffer alterations with the constant use or the environment where the experimental tests occur. In this case, the identification techniques will be borrowed from (LUZ NETTO, 2018). At the end, the model will be validated by comparing the simulation signals with the experimental measurements. For the second plant, an active suspension, we will adopt the model provided by the Quanser company, since its dynamics is already stable.

3.1 Mathematical Models

In this section, we present the equations that will describe the behavior of the two mechanical plants to be considered in this thesis.

3.1.1 Inverted Pendulum

From the Figure 3.1, we appreciate the main parts of the inverted pendulum, identified as IP02 system, which is formed by a motor-driven car an a pendulum attached to it. Additionally, we add a schematic diagram in Figure 3.2 that shows the main variables that will be considered to describe the dynamics of the IP02 system.

Linear and Nonlinear model

The equations and developments that can be derived from the schematic of Figure 3.2 are available in (LUZ NETTO, 2018). From this reference, the nonlinear model of the system is presented as follows

$$(M_p + \mathcal{M}_{eq})\ddot{x}_c + \mathcal{B}_{eq}\dot{x}_c - M_p l_p \cos(\theta)\ddot{\theta} + M_p l_p \sin(\theta)\dot{\theta}^2 = \mathcal{A}_{eq} V_m \tag{3.1}$$

$$(M_p l_p^2 + J_p)\ddot{\theta} + B_p\dot{\theta} - M_p l_p \cos(\theta)\ddot{x}_c - M_p l_p g \sin(\theta) = 0 \tag{3.2}$$

where the equivalent mass is given by

$$\mathcal{M}_{eq} = M_c + \frac{\eta_g k_g^2 J_m}{r_{pm}^2} \tag{3.3}$$

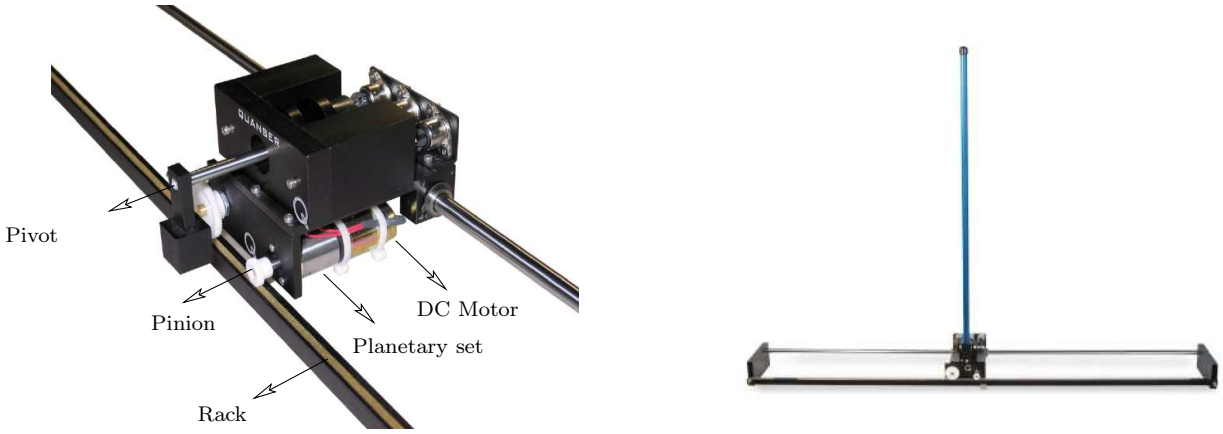

Figure 3.1: IP02 system, obtained from (QUANSER, 2012b)

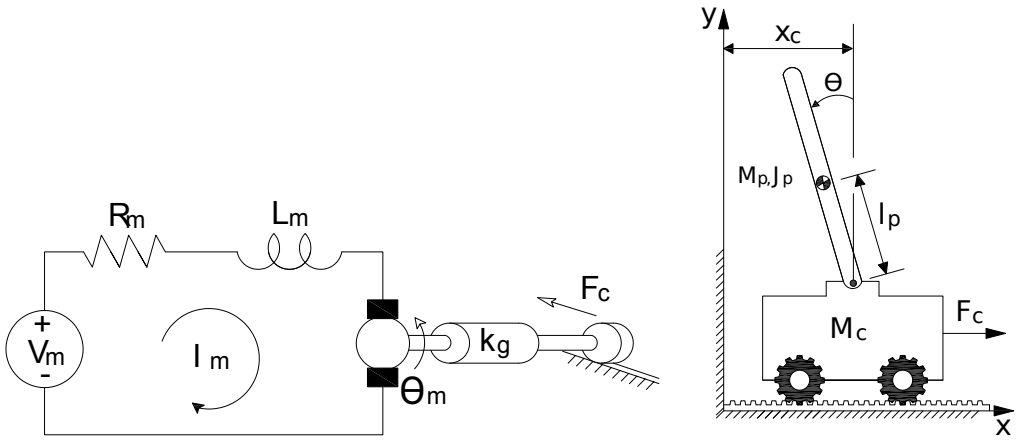

Figure 3.2: Diagram of the car-pendulum set

the equivalent viscous friction is

$$\mathcal{B}_{eq} = B_c + \frac{\eta_m \eta_g k_g^2 k_t k_m}{r_{pm}^2 R_m} \tag{3.4}$$

and, finally, the quantity

$$\mathcal{A}_{eq} = \frac{\eta_m \eta_g k_g k_t}{r_{pm} R_m} \tag{3.5}$$

represents the actuation gain. In the Table 4.1 we summarize the parameters that are involved in the equations (3.1) - (3.2)

The linearized model with respect to the operating point $(x_0, \theta_0, \dot{x}_0, \dot{\theta}_0) = (0, 0, 0, 0)$ is given by the equations

$$(M_p + \mathcal{M}_{eq})\ddot{x}_c + \mathcal{B}_{eq}\dot{x}_c - M_p l_p \ddot{\theta} = \mathcal{A}_{eq} V_m \tag{3.6}$$

$$(M_p l_p^2 + J_p)\ddot{\theta} + B_p \dot{\theta} - M_p l_p g \theta - M_p l_p \ddot{x}_c = 0 \tag{3.7}$$

and will be widely used for identification and control design.

Defining the state vector as being $x = [x_c \quad \theta \quad \dot{x} \quad \dot{\theta}]'$ and the control input as $u = V_m$, the system (3.6)-(3.7) can be described by the state space representation

$$\dot{x}(t) = Ax(t) + Bu(t), x(0) = x_0 \tag{3.8}$$

Symbol	Description	Units
B_p	Equivalent viscous damping coefficient of the pendulum	N.m.s/rad
M_p e l_p	Mass and length of the pendulum	kg
J_p e J_m	Moment of inertia of the pendulum and the motor	kg.m^2
R_m e L_m	Motor armature resistance and motor armadure inductance	Ω , mH
k_m e k_t	Motor back-emf and motor current-torque constant	V/(rad/s), N.m/A
η_m e η_g	Motor and planetary gearbox efficiency	$--$
K_g e r_{pm}	Planetary gearbox gear ratio and Motor pinion radius	$--$,m
M_c e B_c	Mass of cart and Equivalent viscous damping coefficient of the car	kg, N.m.s/rad

Table 3.1: Main parameters associated with the IP02 system

where matrices A and B are given by

$$A = \frac{1}{J_t}\begin{bmatrix} 0 & 0 & J_T & 0 \\ 0 & 0 & 0 & J_T \\ 0 & M_p^2 l_p^2 g & -\mathcal{B}_{eq}(M_p l_p^2 + J_p) & -B_p M_p l_p \\ 0 & M_p l_p g(\mathcal{M}_{eq} + M_p) & -\mathcal{B}_{eq} M_p l_p & -B_p(\mathcal{M}_{eq} + M_p) \end{bmatrix} \tag{3.9}$$

$$B = \frac{\mathcal{A}_{eq}}{J_T}\begin{bmatrix} 0 \\ 0 \\ M_p l_p^2 + J_p \\ M_p l_p \end{bmatrix} \tag{3.10}$$

with $J_T = \mathcal{M}_{eq}(M_p l_p^2 + J_p) + J_p M_p$.

Identification of Physical Parameters

Due to the necessity of obtaining a suitable mathematical model that describes with precision the dynamics of the system, our goal is to identify parameters related to the viscous friction coefficients B_p , B_c and the efficiencies η_m and η_g of the IP02 system. More specifically, we want to identify the parameters $\mathcal{M}_{eq}$, $\mathcal{B}_{|\text{II}}$, $\mathcal{A}_{eq}$, B_p and J_p. The focus on these parameters comes from their strong dependence on external factors, like the rail wear and the experimental environment, while the rest of the quantities M_c, M_p and l_p may be easily measured. The experimental tests done during the identification process will also allow to identify nonlinearities that have not been taken into account during the modeling.

To identify the mentioned parameters we need to change the operating point for $(x_c, \alpha) = (0, \theta + \pi)$ which is stable, differently from the previous one. In this situation, the pendulum is not inverted and is placed in an equilibrium position. Naturally, the linearized model becomes

$$(M_p + \mathcal{M}_{eq})\ddot{x}_c + \mathcal{B}_{eq}\dot{x}_c + M_p l_p \ddot{\alpha} = \mathcal{A}_{eq} V_m \tag{3.11}$$

$$(M_p l_p^2 + J_p)\ddot{\alpha} + B_p\dot{\alpha} + M_p l_p g\alpha + M_p l_p \ddot{x}_c = 0 \tag{3.12}$$

described now in terms of α.

Identification of the car/motor set

Our goal at this moment is to identify the parameters $\mathcal{M}_{eq}$, $\mathcal{B}_{|\text{II}}$ and $\mathcal{A}_{eq}$. From the equations (3.11)-(3.12) it is possible to notice that the group car/motor and the pendulum can be analyzed

separately. In this case, we may uncouple the pendulum from the car, making $M_p = 0$ in equation (3.11), obtaining the motion equation of the car, which assumes the format:

$$\mathcal{M}_{eq}\ddot{x}_c + \mathcal{B}_{eq}\dot{x}_c = \mathcal{A}_{eq}V_m \tag{3.13}$$

In the physical system, this adaptation is made simply by removing of the pendulum from the support rod. Defining $\dot{x}_c = v_c$, the linear speed of the car, we obtain a first order differential linear equation given by

$$\tau\dot{v}_c + v_c = \kappa_0 V_m \tag{3.14}$$

with

$$\kappa_0 = \frac{\mathcal{A}_{eq}}{\mathcal{B}_{eq}},\ \tau = \frac{\mathcal{M}_{eq}}{\mathcal{B}_{eq}} \tag{3.15}$$

The response of this system for an input $V_m(t) = \upsilon_0,\ \forall t \geq 0$, is given by

$$v_c(t) = \kappa_0\upsilon_0(1 - e^{\frac{t}{\tau}}) \tag{3.16}$$

which allows us to determine the time constant τ and the gain κ_g by the following procedure based on two simple steps:

- For $t \to \infty$, it is simple to verify that $\kappa_0\upsilon_0$ is the steady-state value of $v_c(t)$
- For $t = \tau$ we have $v_c(\tau) = \kappa_0(1 - e^{-1})$ and, consequently, τ is the instant in which the response $v_c(t)$ reaches the 63% of its steady-state value.

Notice that from this test, it is not possible to find separately the three parameters of interest $\mathcal{A}_{eq}$, $\mathcal{M}_{eq}$ and $\mathcal{B}_{eq}$. This difficulty may be circumvented with the support of an extra experimental test of the same type. The idea is to couple a known mass M_k to the car in such a way that the dynamic equation (3.14) be identical but with a new time constant

$$\tau' = \frac{\mathcal{M}_{eq} + M_k}{\mathcal{B}_{eq}} \tag{3.17}$$

which, along with (3.15) allow us to determine

$$\mathcal{B}_{eq} = \frac{M_k}{\tau' - \tau},\ \mathcal{M}_{eq} = \mathcal{B}_{eq}\tau,\ \mathcal{A}_{eq} = \mathcal{B}_{eq}\kappa_0 \tag{3.18}$$

We have submitted the IP02 system to these experimental tests using an additional mass of $M_k = 0.369$ [kg]. The identification has been done for a range of amplitudes from $2.5[V]$ to $4[V]$ with an increment of $0.5[V]$ between tests, being the value presented in Table 3.2 obtained as the mean of the values.

Identified parameters - Car/Motor			
E. IP02	$\mathcal{A}_{eq}$ [N/V]	$\mathcal{M}_{eq}$ [kg]	$\mathcal{B}_{eq}$ [kg/s]
N ^{o} 1	1.0274	1.1570	6.2542

Table 3.2: Identified parameters of the car

In order to validate the identified model, we have obtained the response $v_c(t)$ for a step input of 0.7 [V] and 3 [V] and compared the experimental measurements with the response of (3.14) with the identified parameters. Figure 3.5 presents these responses. Notice that for an input of

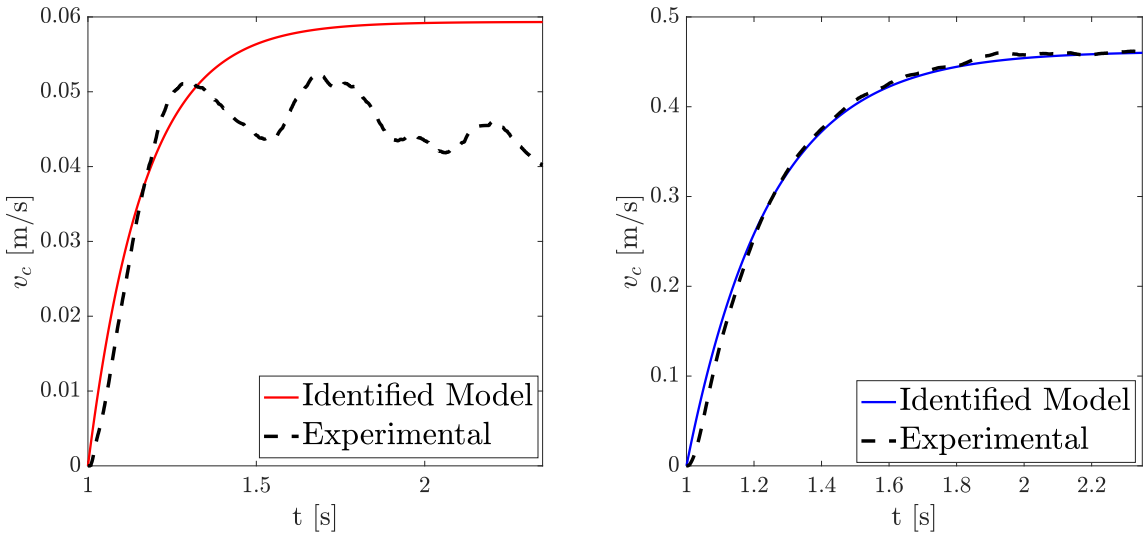

Figure 3.3: Car response to a step input of 0.7 [V] (left) and 3 [V] (right)

0.7 [V] of amplitude, the response $v_c t$ is not satisfactory due to the influence of external factors as the encoder cable and the Coulomb friction. Both phenomena have not been considered in the modeling process. However, for greater amplitudes, the identified model has presented a response very similar to that provided by the real system, indicating that the influence of these nonlinearities and perturbations is considerably attenuated. This validates the identification process and confirms that the identified parameters represent with precision the real system.

Pendulum Identification

To identify the parameters B_p and J_p present in equation (3.12) we may lock up the movement of the car and consider only the oscillation of the pendulum. In this case, $\ddot{x}_c$ is eliminated of the equation (3.12), which can be rewritten as

$$\ddot{\alpha} + 2\xi\omega_n\dot{\alpha} + \omega_n^2\alpha = 0 \tag{3.19}$$

where

$$2\xi\omega_n = \frac{B_p}{(M_p l_p^2 + J_p)}, \quad \omega_n^2 = \frac{M_p l_p g}{(M_p l_p^2 + J_p)} \tag{3.20}$$

From the determination of ω_n and ξ, it is possible to obtain the desired parameters. The next developments are based on (GEROMEL; KOROGUI, 2001). In fact, considering that the pendulum evolves from the rest with the initial condition $\alpha(0) = \alpha_0$, applying the Laplace Transformation in (3.19) we obtain:

$$\begin{aligned} \hat{\alpha}(s) &= \frac{\alpha_0(s + 2\xi\omega_n)}{s^2 + 2\xi\omega_n s + \omega_n^2} \\ &= \alpha_0\left(\frac{s + \xi\omega_n}{(s + \xi\omega_n)^2 + \omega_d^2} + \left(\frac{\xi\omega_n}{\omega_d}\right)\frac{\omega_d}{(s + \xi\omega_n)^2 + \omega_d^2}\right) \end{aligned} \tag{3.21}$$

in which $\omega_d = \omega_n\sqrt{1 - \xi^2}$ is the angular frequency of the damped oscillation. The inverse Laplace

transform allows us to find the following time response

$$\begin{aligned} \alpha(t) &= \frac{\alpha_0 e^{-\xi\omega_n t}}{\omega_d}(\omega_d \cos(\omega_d t) + \xi\omega_n \sin(\omega_d t)) \\ &= \frac{\alpha_0 e^{-\xi\omega_n t}}{\sin(\phi)} \sin(\omega_d t + \phi) \end{aligned} \tag{3.22}$$

where

$$\text{tg}(\phi) = \frac{\omega_d}{\xi\omega_n} = \sqrt{\xi^{-2} - 1} \tag{3.23}$$

for $0 < \xi < 1$. It is important to note that, from the equation (3.22) , the derivative of $\alpha(t)$ with respect to time allows us to observe that the points of maximum and minimum of the function satisfy the equality $\text{tg}(\omega_d t + \phi) = \text{tg}(\phi)$ and, therefore

$$\omega_d t_i = i\pi, i = 0, 1, 2 \ldots \tag{3.24}$$

Then, taking into account that $\omega_d(t_{i+1} - t_i) = \pi$, we have that the mean value related to m points of maximum and minimum obtained from the measurement of the angular displacement provides the relation

$$\omega_d = \frac{(m-1)\pi}{\sum_{i=1}^{m-1}(t_{i+1} - t_i)} \tag{3.25}$$

Applying the same time instants in the equation (3.21), we obtain:

$$\alpha(t_i) = \alpha_0 e^{-\xi\omega_n t_i}(-1)^i, i = 0, 1, 2, \ldots \tag{3.26}$$

which indicates that the points of maximum and minimum satisfy the relation

$$\frac{|\alpha(t_{i+1})|}{|\alpha(t_i)|} = e^{-\xi\omega_n(t_{i+1} - t_i)} = e^{-\pi/tg(\phi)} \tag{3.27}$$

Finally, in an equivalent way, after algebraic manipulations, we reach the equality

$$\text{tg}(\phi) = \frac{(m-1)\pi}{\sum_{i=1}^{m-1}(\ln(|\alpha(t_i|) - \ln(|\alpha(t_{i+1}|))} \tag{3.28}$$

Note that, after determining ω_d from the (3.25), using the equation (3.28) along with (3.23) allows us to obtain the value of ξ and, consequently, of the natural frequency ω_n. With these values we can determined

$$J_p = \frac{M_p l_p g}{\omega_n^2} - Mpl_p^2, \quad B_p = 2\xi\omega_n(M_p l_p^2 + J_p) \tag{3.29}$$

In the physical system, the car is fixed and the pendulum evolves from the initial condition $\alpha_0 = -0.6243$ [rad]. Using the values of maximum and minimum of $\alpha(t)$, we have determined ξ, ω_n and, consequently, the desired parameters B_p and J_p as shown in Table 3.3.

Identified parameters - Pendulum				
E. IP02	ξ	ω_n [rad/s]	B_p [kg.m^2.rad/s]	J_p [kg.m^2]
N ^{o} 1	0.0028	4.7201	0.00087	0.0084

Table 3.3: Identified parameters of the pendulum

Figure (3.4) compares the measured angular displacement with the one obtained from the model identified. Notice that the identified parameters precisely represented the behavior of the real system, since the responses of the identified and physical models were very similar. However, after 80 [s] both graphs have presented a slightly different behavior, since the physical system goes to the origin more rapid than the identified system. This fact is related to the omission of the Coulomb friction force in the model, which acts over the pendulum when the speed changes its direction and whose influence is more important when the velocity becomes smaller.

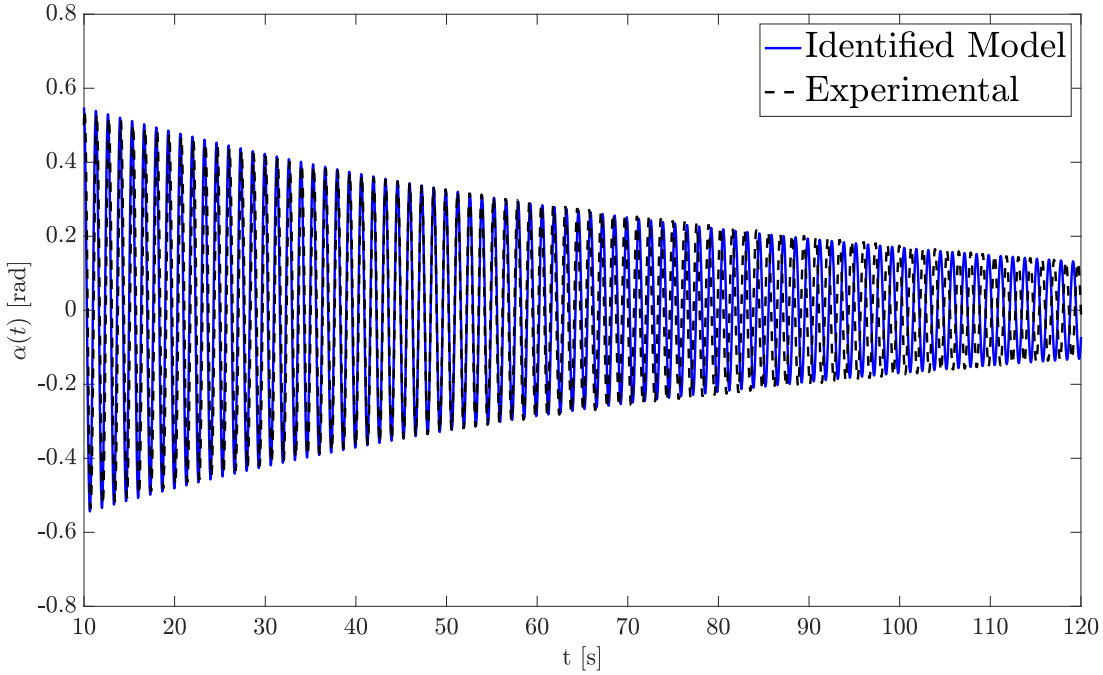

Figure 3.4: Angular displacement of the pendulum

Validation

The identified parameters are presented in Table 3.4 as well as a comparison with the values provided by the Quanser company. Figure 3.5 presents the responses to a square wave with frequency of 1.5 [Hz] and amplitude of 4 [V] applied to $V_m(t)$. It has been considered the real system, the identified model and the model obtained with parameters provided by Quanser®. It is remarkable that the identification of the system allowed us to obtain of a more precise model when compared to the one provided by the company.

Identified variables *versus* provided by Quanser				
E. IP02 N1	Quanser	Identified	Unit	Variation
$\mathcal{A}_{eq}$	1.0717	1.0274	[N/V]	−5%
$\mathcal{B}_{eq}$	5.4	6.2542	[kg/s]	16%
$\mathcal{M}_{eq}$	1.2863	1.1570	[kg]	−10%
B_p	0.0024	0.00087	[kg.m^2.rad/s]	−64%
J_p	0.00788	0.0084	[kg.m^2]	7%

Table 3.4: Comparison among the results

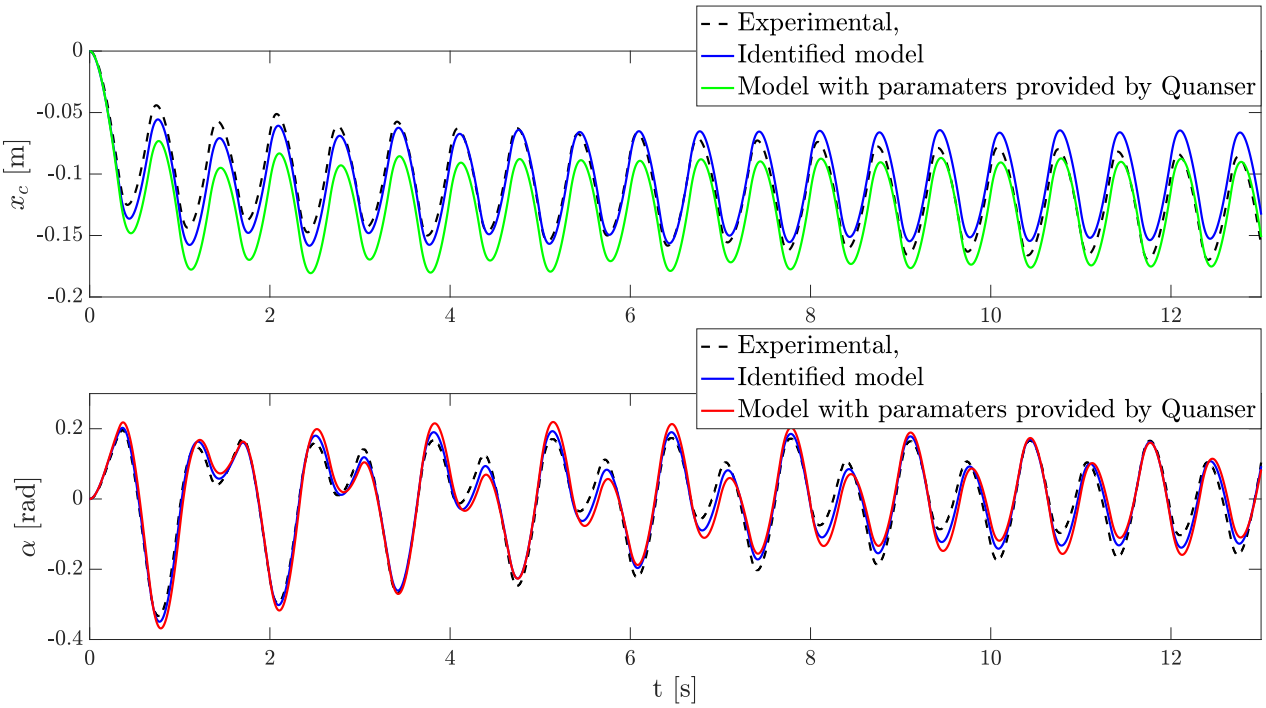

Figure 3.5: Response comparison for a square wave with 1.5 [Hz] and 4 [V]

With the identified parameters, we have obtained the linearized model (3.8) with matrices

$$A = \begin{bmatrix} 0 & 0 & 1 & 0 \\ 0 & 0 & 0 & 1 \\ 0 & 1.3931 & -5.1494 & -0.0016 \\ 0 & 25.4435 & -11.6949 & -0.0297 \end{bmatrix}, B = \begin{bmatrix} 0 \\ 0 \\ 0.8459 \\ 1.9212 \end{bmatrix} \tag{3.30}$$

which will be used in the next chapter for control design purposes. The next section is dedicated to obtain the mathematical model of the active suspension.

3.2 Suspension model

Figure 3.6 shows to the left the real active suspension used for the experimental tests and to the right its schematic diagram that presents the main variables, as well as the reference system used to describe its dynamics. Table 3.5 presents the description of the suspension parameters together with their units. Based on this diagram and defining the state vector as being $x = [(z_s - z_{us})\ \dot{z_s}\ (z_{us} - z_r)\ \dot{z_{us}}]'$, the control input as $u = F_c$ and the external input as $w = \dot{z}_r$, the suspension is described by the following state space realization:

$$\dot{x}(t) = Ax(t) + Bu(t) + Hw(t),\ x(0) = x_0 \tag{3.31}$$

with matrices

$$A = \begin{bmatrix} 0 & 1 & 0 & -1 \\ -\frac{K_s}{M_s} & -\frac{B_s}{M_s} & 0 & \frac{B_s}{M_s} \\ 0 & 0 & 0 & 1 \\ \frac{K_s}{M_{us}} & \frac{B_s}{M_{us}} & -\frac{K_{us}}{M_{us}} & -\frac{B_s+B_{us}}{M_{us}} \end{bmatrix}, B = \begin{bmatrix} 0 \\ \frac{1}{M_s} \\ 0 \\ -\frac{1}{M_{us}} \end{bmatrix}, H = \begin{bmatrix} 0 \\ 0 \\ -1 \\ \frac{B_{us}}{M_{us}} \end{bmatrix} \tag{3.32}$$

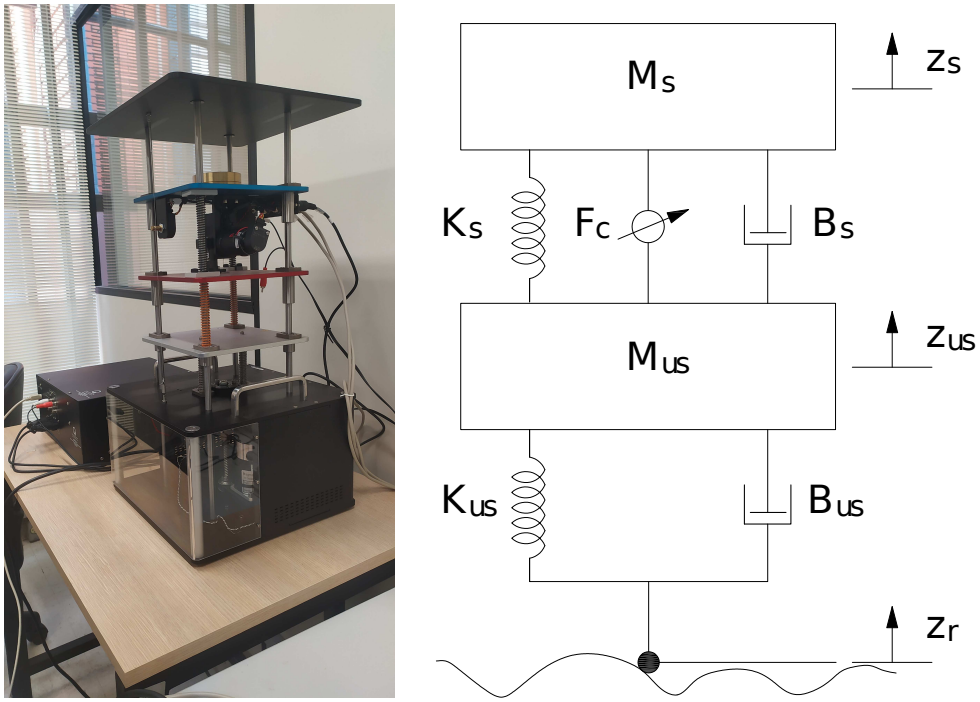

Figure 3.6: Active suspension from Quanser and its schematic

Symbol	Description	Units
M_s and M_{us}	Sprung and unsprung mass	kg
B_s andB_{us}	Spring stiffness coefficients	N.s/m
K_s and K_{us}	Damping coefficients	N/m
z_r	Displacement of the gray plate	m
z_{us}	Displacement of the red plate	m
z_s	Displacement of the blue plate	m
F_c	Force provided by the actuator	N

Table 3.5: Main parameters associated to the active suspension

Considering the numerical values borrowed from reference (QUANSER, 2012a) as being $M_s = 2.45$ [kg], $M_{us} = 1$ [kg], $K_s = 900$ [N/m], $K_{us} = 2300$ [N/m], $B_s = 7.5$ [N.s/m] and $B_{us} = 5$ [N.s/m], we obtain that (3.31) is given as follows

$$A = \begin{bmatrix} 0 & 1 & 0 & -1 \\ -367.35 & -3.06 & 0 & 3.06 \\ 0 & 0 & 0 & 1 \\ 900 & 7.50 & -2300 & -12.50 \end{bmatrix}, B = \begin{bmatrix} 0 \\ 0.4082 \\ 0 \\ -1 \end{bmatrix}, H = \begin{bmatrix} 0 \\ 0 \\ -1 \\ 5 \end{bmatrix} \tag{3.33}$$

which will be very useful for the control purpose to be developed in the next chapter.

3.3 Final Considerations

This chapter has been dedicated to the description of the mechanical systems to be considered in the next chapter for cooperative control, via communication networks. More specifically, we have presented the nonlinear and linear models of the inverted pendulum, which is unstable, as well as the model of the suspension, which is already stable. In order to obtain a more precise pendulum model we have identified some of its parameters and validated the identified model, while for the suspension we have used the parameters provided in the manual (QUANSER, 2012a).

Chapter 4

Cooperative Control

This chapter presents the main results of this thesis. It treats cooperative control, through a communication network with limited bandwidth, of several linear time invariant plants. More specifically, the main goal is to design a control law that cooperatively shares the resources among the LTI systems, assuring global asymptotic stability and an $\mathcal{H}_2$ guaranteed performance index. A coordinator, represented mathematically by a switching rule, must select at each interval of time the LTI system to receive the updated control signal, while the others maintain the previously received one. This problem has already been treated in (SOUSA; GEROMEL; DEAECTO, 2015) and (LUZ NETTO, 2018) but through conditions based on Lyapunov-Metzler inequalities, which are nonconvex and very difficult to solve for an arbitrary number of plants. The main contribution of this thesis is to obtain alternative conditions described in terms of linear matrix inequalities, which are simple to solve by readily available tools. We have compared our methodology with the existent one by means of an academical example. Moreover, we have validated the proposed technique by making the cooperative control of the two mechanical plants, whose models and discussions have been presented in the previous chapter.

4.1 Problem Statement

First, let us consider a Networked Control System (NCS) composed by N LTI plants that must be simultaneously controlled in a cooperative perspective. These plants have the following state-space realization in the continuous-time domain

$$\begin{aligned} \dot{x}_i(t) &= A_i x_i(t) + B_i u_i(t) + H_i w_i(t), x_i(0) = 0 \\ z_i(t) &= C_i x_i(t) + D_i u_i(t) \end{aligned} \tag{4.1}$$

where for all $t \geq 0$ and all $i \in \mathbb{K}$, $x_i(\cdot) \in \mathbb{R}^{n_x}$, $u_i(\cdot) \in \mathbb{R}^{n_u}$, $w_i(\cdot) \in \mathbb{R}^{n_w}$ and $z_i(\cdot) \in \mathbb{R}^{n_z}$ are the state, the control input, the exogenous input and the controlled output, respectively. Let us assume that the external input is of impulsive type $w_i = e_q \delta(t)$, in which e_q is the q-th column of the n_w order identity matrix. Moreover, the control law $u_i(t)$ must satisfy the following design requirements

- **Channel bandwidth limitation** is implemented by adopting the sampled-data control strategy

$$u_i(t) = u_i(t_n) = u_i[n],\ t \in [t_n, t_{n+1}) \tag{4.2}$$

for $i \in \mathbb{K}$ and where $t_{n \in \mathbb{N}}$ are successive sampling instants such that $t_0 = 0$, $t_{n+1} - t_n = h > 0$, and $\lim_{n \to \infty} t_n = \infty$. The sampling frequency $1/h$ characterizes the bandwidth of the transmission channel.

- **Cooperative resource sharing** indicates that at any sampling time $t_n \geq 0$ the transmission channel is used to control only the plant defined by the index $\sigma[n] \in \mathbb{K}$ through the adoption of a state feedback control law of the form

$$u_i[n] = \begin{cases} K_i u_i[n-1] + L_i x_i[n] & , \ i = \sigma[n] \\ u_i[n-1] & , \ i \neq \sigma[n] \end{cases} \tag{4.3}$$

  where (K_i, L_i) are matrix gains of compatible dimensions to be determined, $\forall i \in \mathbb{K}$. These variables must be designed in order to improve the closed-loop system performance.

- **$\mathcal{H}_2$ performance index** is defined as being

$$J_2(\sigma) = \inf_{K_i, L_i, \sigma \in \Omega} \sum_{i=1}^{N} \sum_{q=1}^{n_w} \int_0^\infty z_i^q(t)' z_i^q(t) dt \tag{4.4}$$

  where Ω is the set of all stabilizing switching functions. The controlled output $z_i^q(t)$ is the response of the i-th plant to the impulse response $w_i = e_q \delta(t)$, in which as already mentioned e_q is the q-th column of the n_w order identity matrix.

Notice that the control strategy (4.3) keeps the previously received control signal $u_i[n] = u_i[n-1]$ for the plants where $i \neq \sigma[n] \in \mathbb{K}$, since the communication channel is dedicated to the i-th plant. This plant, by its turn, receives the updated state feedback control law $u_i[n] = K_i u_i[k-1] + L_i x_i[n]$, since $i = \sigma[n]$. Hence, the switching law is responsible by choosing at each time $t_n \geq 0$ which plant must receive the updated control signal.

4.1.1 Switched System Modeling

First, let us notice that due to the impulsive external input $w_i = e_q \delta(t)$, system (4.1) can be written alternatively as

$$\begin{aligned} \dot{x}_i(t) &= A_i x_i(t) + B_i u_i(t), x_i(0) = H_i e_q \\ z_i(t) &= C_i x_i(t) + D_i u_i(t) \end{aligned} \tag{4.5}$$

Now, defining the scalar variable $\delta_{ij} \in \{0, 1\}$ for all $(i, j) \in \mathbb{K} \times \mathbb{K}$ as being

$$\delta_{ij} = \begin{cases} 1 & , \ i = \sigma[n] \\ 0 & , \ i \neq \sigma[n] \end{cases} \tag{4.6}$$

we can rewrite the control signal (4.3) as follows

$$u_i[n] = (1 - \delta_{i\sigma}) u_i[n-1] + \delta_{i\sigma}(K_i u_i[n-1] + L_i x_i[n]) \tag{4.7}$$

which will be widely used afterwards.

The fact that this control signal is constant inside the entire time interval defined by two successive sampling instants, as presented in (4.2), makes possible to determine an equivalent discrete-time system with state space realization

$$\begin{aligned} x_i[n+1] &= A_{ih} x_i[n] + B_{ih} u_i[n], \ x_i[0] = H_i e_q \\ z_i[n] &= C_{ih} x_i[n] + D_{ih} u_i[n], \end{aligned} \tag{4.8}$$

This system is equivalent to (4.5) in the sense that the equality

$$\int_0^\infty z_i(t)'z_i(t)dt = \sum_{k\in\mathbb{N}} z_i[n]'z_i[n] \tag{4.9}$$

is preserved, see references (SOUZA et al., 2014) and (CHEN; FRANCIS, 2012) for more details about this discretization. Defining the augmented matrices

$$F_i = \begin{bmatrix} A_i & B_i \\ 0 & 0 \end{bmatrix}, G_i = \begin{bmatrix} C_i & D_i \end{bmatrix} \tag{4.10}$$

matrices (A_{ih}, B_{ih}) are obtained from the identity

$$e^{F_i h} = \begin{bmatrix} A_{ih} & B_{ih} \\ 0 & I \end{bmatrix} \tag{4.11}$$

whereas the output matrices (C_{ih}, D_{ih}) follows from

$$\int_0^h e^{F_i' t} G_i G_i' e^{F_i t} dt = \begin{bmatrix} C_{ih}' \\ D_{ih}' \end{bmatrix} \begin{bmatrix} C_{ih}' & D_{ih}' \end{bmatrix}' \tag{4.12}$$

Defining the augmented state space vector $\eta_i[n] = [x_i[n]' \quad u_i[n-1]']'$ and connecting the control input (4.7) to the system (4.8), we obtain the closed-loop system given by

$$\begin{aligned} \eta_i[n+1] &= (\mathcal{A}_{i\sigma} + \mathcal{B}_{i\sigma}\mathcal{K}_i)\eta_i[n],\ \eta_{i0} = \mathcal{H}_i e_q \\ z_i[n] &= (\mathcal{C}_{i\sigma} + \mathcal{D}_{i\sigma}\mathcal{K}_i)\eta_i[n] \end{aligned} \tag{4.13}$$

in which $\mathcal{H}_i = [H_i' \quad 0]'$, the gain is $\mathcal{K}_i = [L_i \quad K_i]$ and the augmented matrices are

$$\mathcal{A}_{i\sigma} = \begin{bmatrix} A_{ih} & (1-\delta_{i\sigma})B_{ih} \\ 0 & (1-\delta_{i\sigma})I \end{bmatrix}, \mathcal{B}_{i\sigma} = \begin{bmatrix} \delta_{i\sigma}B_{ih} \\ \delta_{i\sigma}I \end{bmatrix}, \mathcal{C}_{i\sigma} = \begin{bmatrix} C_{ih} & (1-\delta_{i\sigma})D_{ih} \end{bmatrix}, \mathcal{D}_{i\sigma} = \begin{bmatrix} \delta_{i\sigma}D_{ih} \end{bmatrix} \tag{4.14}$$

which depends in two matrices gains (L_i, K_i) for all $i \in \mathbb{K}$. In order to present the system in a clearer way we can express the closed-loop system for $i = \sigma[n]$ as follows

$$\begin{aligned} \eta_i[n+1] &= \begin{bmatrix} A_{ih} + B_{ih}L_i & B_{ih}K_i \\ L_i & K_i \end{bmatrix} \eta_i[n], \eta_{i0} = \mathcal{H}_i e_q \\ z_i[n] &= \begin{bmatrix} C_{ih} + D_{ih}L_i & D_{ih}K_i \end{bmatrix} \eta_i[n] \end{aligned} \tag{4.15}$$

and for $i \neq \sigma[n]$ as follows

$$\begin{aligned} \eta_i[n+1] &= \begin{bmatrix} A_{ih} & B_{ih} \\ 0 & I \end{bmatrix} \eta_i[n], \eta_{i0} = \mathcal{H}_i e_q \\ z_i[n] &= \begin{bmatrix} C_{ih} & D_{ih} \end{bmatrix} \eta_i[n] \end{aligned} \tag{4.16}$$

Notice that whenever the pair (A_{ih}, B_{ih}) is stabilizable there always exist state feedback gains (K_i, L_i) such that the closed-loop matrix of (4.15) is stable, which is clear by making $K_i = 0$. However, all other plants $i \neq \sigma[n]$ will be unstable, since from equation (4.16) their models presents at least n_u unitary common eigenvalues. Hence, we can conclude that the switching rule is essential to control the overall networked control systems mainly because the $\mathcal{H}_2$ criterion (4.4) depends on the controlled output of all plants and, consequently, the control must be able to stabilize all of them by taking into account the channel transmission constraints under consideration.

4.1.2 Switching Control Design

In this section, we aim to design a switching control for resource allocation for the switched linear system (4.13) supposing, at this first moment, that the gain $\mathcal{K}_i$ is given. Hence, the system under consideration can be rewritten as

$$\eta_i[n+1] = \tilde{\mathcal{A}}_{i\sigma}\eta_i[n],\ \ \eta_i[0] = \mathcal{H}_i e_q \tag{4.17}$$

$$z_i[n] = \tilde{\mathcal{C}}_{i\sigma}\eta_i[n] \tag{4.18}$$

with $\tilde{\mathcal{A}}_{ij} = \mathcal{A}_{ij} + \mathcal{B}_{ij}\mathcal{K}_i$ and $\tilde{\mathcal{C}}_{ij} = \mathcal{C}_{ij} + \mathcal{D}_{ij}\mathcal{K}_i$. Let us consider the quadratic time-varying Lyapunov function candidate

$$V(\eta_i[n], n) = \sum_{i=1}^{N} \eta_i[n]'\mathcal{P}_i[n]\eta_i[n] \tag{4.19}$$

where N represents the number of plants and $\mathcal{P}[n] = \mathcal{P}[k(n)]$ is a periodic positive definite matrix. As in Chapter 2 this matrix presents period equal to κ and satisfies the boundary conditions $\mathcal{P}[0] = \mathcal{P}[\kappa]$. The next theorem presents the conditions for the control design of a globally asymptotically state-dependent switching function for the system (4.17)-(4.18).

Theorem 4.1 *For a given positive scalar $1 \leq \kappa \in \mathbb{N}$, assume that there exist vectors $\lambda[n] \in \Lambda$ and matrices $\mathcal{P}[n] > 0$ satisfying the inequalities*

$$\sum_{j=1}^{N} \lambda_j[n]\Big(\tilde{\mathcal{A}}_{ij}'\mathcal{P}_i[n+1]\tilde{\mathcal{A}}_{ij} - \mathcal{P}_i[n] + \tilde{\mathcal{C}}_{ij}'\tilde{\mathcal{C}}_{ij}\Big) < 0 \tag{4.20}$$

for all $i \in \mathbb{K}$ and $n = 0, \cdots, \kappa-1$, respecting the boundary condition $\mathcal{P}[0] = \mathcal{P}[\kappa]$. Then, the state-dependent switching function

$$\sigma(\eta) = \arg\min_{j\in\mathbb{K}} \sum_{i=1}^{N} \eta_i[n]'(\tilde{\mathcal{A}}_{ij}'\mathcal{P}_i[k(n)+1]\tilde{\mathcal{A}}_{ij} + \tilde{\mathcal{C}}_{ij}'\tilde{\mathcal{C}}_{ij})\eta_i[n] \tag{4.21}$$

assures the global asymptotic stability of the system (4.17)-(4.18) and satisfies the guaranteed cost

$$\sum_{i\in\mathbb{K}} \|z_i\|_2^2 < \sum_{i\in\mathbb{K}} \eta_i[0]'\mathcal{P}_i[0]\eta_i[0] \tag{4.22}$$

Proof: Defining $\Delta V(\eta, n) = V(\eta, n+1) - V(\eta, n)$, we have that in the time interval $0 \leq n \leq \kappa-1$, the inequality (4.20) together with the switching function (4.21), yield

$$\begin{aligned}
\Delta V(\eta, n) &= \sum_{i=1}^{N} \eta_i[n]'\left(\tilde{\mathcal{A}}_{i\sigma}'\mathcal{P}_i[n+1]\tilde{\mathcal{A}}_{i\sigma} - \mathcal{P}_i[n] + \tilde{\mathcal{C}}_{i\sigma}'\tilde{\mathcal{C}}_{i\sigma}\right)\eta_i[n] - \sum_{i=1}^{N} z_i[n]'z_i[n] \\
&= \min_{j\in\mathbb{K}} \sum_{i=1}^{N} \eta_i[n]'\left(\tilde{\mathcal{A}}_{ij}'\mathcal{P}_i[n+1]\tilde{\mathcal{A}}_{ij} - \mathcal{P}_i[n] + \tilde{\mathcal{C}}_{ij}'\tilde{\mathcal{C}}_{ij}\right)\eta_i[n] - \sum_{i=1}^{N} z_i[n]'z_i[n] \\
&= \min_{\lambda[n]\in\Lambda} \sum_{i=1}^{N} \eta_i[n]'\left(\sum_{j=1}^{N} \lambda_j[n]\left(\tilde{\mathcal{A}}_{ij}'\mathcal{P}_i[n+1]\tilde{\mathcal{A}}_{ij} - \mathcal{P}_i[n] + \tilde{\mathcal{C}}_{ij}'\tilde{\mathcal{C}}_{ij}\right)\right)\eta_i[n] - \sum_{i=1}^{N} z_i[n]'z_i[n] \\
&\leq \sum_{i=1}^{N} \eta_i[n]'\left(\sum_{j=1}^{N} \lambda_j[n]\left(\tilde{\mathcal{A}}_{ij}'\mathcal{P}_i[n+1]\tilde{\mathcal{A}}_{ij} - \mathcal{P}_i[n] + \tilde{\mathcal{C}}_{ij}'\tilde{\mathcal{C}}_{ij}\right)\right)\eta_i[n] - \sum_{i=1}^{N} z_i[n]'z_i[n] \\
&< -\sum_{i=1}^{N} z_i[n]'z_i[n]
\end{aligned} \tag{4.23}$$

where the second equality is due to the switching function and the third one comes from a known property of the minimum operator. The first inequality is also a consequence of the minimum operator and last one is due to the validity of the inequality (4.20). Notice that $\Delta V(\eta, n) < -\sum_{i=1}^{N} z_i[n]' z_i[n] < 0$ indicating that the switching function is globally asymptotically stable. Now, summing recursively both sides of this inequality from $n = 0$ to $n \to \infty$, we obtain

$$V(\eta[\infty], \infty) - V(\eta[0], 0) < -\sum_{i=1}^{N} \sum_{n=0}^{\infty} z_i[n]' z_i[n] \tag{4.24}$$

which leads us to the guaranteed cost (4.22) since $V(\eta[\infty], \infty) = 0$ due to the asymptotic stability of the system. The proof is concluded. □

Notice that the condition of Theorem 4.1 is nonconvex due to the product of variables $(\lambda[n], \mathcal{P}[n])$ and, therefore, is extremely difficult to solve. Fortunately, a simplification can be adopted without loss of generally searching $\lambda[n]$ only on the vertices of the simplex $\lambda \in \Lambda_v \subset \Lambda$. This simplification is possible thanks to the switching function (4.21), and allows us to solve the conditions of Theorem 4.1 as the solution of a set of convex subproblems as it will be clear afterwards. At this point, it is important to recall the definitions of the sets $\mathfrak{C}(\kappa)$, $\mathfrak{C}_\ell(\kappa)$ provided just after Theorem 2.3. The next corollary presents this new description together with the $\mathcal{H}_2$ guaranteed cost.

Corollary 4.1 *For a given positive scalar $1 \leq \kappa \in \mathbb{N}$, assume that there exist matrices $\mathcal{P}[n] > 0$ solution of the following optimization problem*

$$J_2(\sigma) < \min_{1 \leq \ell \leq N^\kappa} \inf_{\mathcal{P}[n] > 0} \sum_{i=1}^{N} \mathrm{Tr}(\mathcal{H}_i' \mathcal{P}_i[0] \mathcal{H}_i) \tag{4.25}$$

subject to

$$\tilde{\mathcal{A}}_{ij[n]}' \mathcal{P}_i[n+1] \tilde{\mathcal{A}}_{ij[n]} - \mathcal{P}_i[n] + \tilde{\mathcal{C}}_{ij[n]}' \tilde{\mathcal{C}}_{ij[n]} < 0 \tag{4.26}$$

for all $i \in \mathbb{K}$, $n = 0, \cdots, \kappa - 1$, $j[n] \in \mathfrak{C}_\ell(\kappa)$ with the boundary conditions $\mathcal{P}[0] = \mathcal{P}[\kappa]$. Then, the state-dependent switching function (4.21) assures global asymptotic stability of the system (4.17)-(4.18) and satisfies the $\mathcal{H}_2$ guaranteed cost (4.25).

Proof: The conditions (4.26) can be obtained directly from (4.20) following the same arguments provided in the proof of Corollary 2.1 of Chapter 2. To obtain the guaranteed cost (4.25), let us remember the definition of the $\mathcal{H}_2$ performance index (4.4) and that, from (4.17), we have $\eta_i[0] = \mathcal{H}_i e_q$, which allow us to write

$$\begin{aligned} J_2(\sigma) &= \inf_{K_i, L_i, \sigma \in \Omega} \sum_{i=1}^{N} \sum_{q=1}^{n_w} \|z_i^q\|_2^2 \\ &< \inf_{K_i, L_i, \sigma \in \Omega} \sum_{i=1}^{N} \sum_{q=1}^{n_w} e_q' \mathcal{H}_i' \mathcal{P}[0] \mathcal{H}_i e_q \\ &= \inf_{K_i, L_i, \sigma \in \Omega} \sum_{i=1}^{N} \mathrm{Tr}(\mathcal{H}_i' \mathcal{P}[0] \mathcal{H}_i) \end{aligned} \tag{4.27}$$

which leads us to the guaranteed cost (4.25), concluding thus the proof. □

4.1.3 Joint Design

In this subsection, let us consider that the gains $\mathcal{K}_i,\ \forall i \in \mathbb{K}$ are not given. Our main goal is to jointly design the state feedback gains (L_i, K_i) and the matrices $\mathcal{P}_i[n] > 0$ that will be important for the implementation of the switching function (4.21). The co-design conditions are presented in the next theorem and represent the main contribution of this thesis.

Theorem 4.2 *For a given positive scalar $1 \leq \kappa \in \mathbb{N}$, assume that there exist symmetric matrices $\mathcal{X}_i[n]$, $\mathcal{W}_i$ and generic matrices $\mathcal{Y}_i$, $\mathcal{G}_i$ solution of the following optimization problem*

$$J_2(\sigma) < \min_{1\leq \ell \leq N^\kappa} \inf_{\mathcal{X}_i[\cdot],\mathcal{Y}_i,\mathcal{G}_i,\mathcal{W}_i} \sum_{i\in\mathbb{K}} \mathrm{Tr}(\mathcal{W}_i) \tag{4.28}$$

subject to

$$\begin{bmatrix} \mathcal{G}_i' + \mathcal{G}_i - \mathcal{X}_i[n] & \bullet & \bullet \\ \mathcal{A}_{ij[n]}\mathcal{G}_i + \mathcal{B}_{ij[n]}\mathcal{Y}_i & \mathcal{X}_i[n+1] & \bullet \\ \mathcal{C}_{ij[n]}\mathcal{G}_i + \mathcal{D}_{ij[n]}\mathcal{Y}_i & 0 & I \end{bmatrix} > 0, \quad j[n] = i \tag{4.29}$$

$$\begin{bmatrix} \mathcal{X}_i[n] & \bullet & \bullet \\ \mathcal{A}_{ij[n]}\mathcal{X}_i[n] & \mathcal{X}_i[n+1] & \bullet \\ \mathcal{C}_{ij[n]}\mathcal{X}_i[n] & 0 & I \end{bmatrix} > 0, \quad j[n] \neq i \tag{4.30}$$

$$\begin{bmatrix} \mathcal{W}_i & \bullet \\ \mathcal{H}_i & \mathcal{X}_i[0] \end{bmatrix} > 0 \tag{4.31}$$

for all $i \in \mathbb{K}$, $n = 0, \cdots, \kappa - 1$, and $j[n] \in \mathfrak{C}_\ell(\kappa)$ and the boundary conditions $\mathcal{X}_i[0] = \mathcal{X}_i[\kappa]$, then the switching function (4.21) with $\mathcal{P}_i[\cdot] = \mathcal{X}_i[\cdot]^{-1}$ and the control law (4.4) with $\mathcal{K}_i = \mathcal{Y}_i\mathcal{G}_i^{-1}$ assure (4.17)-(4.18) and satisfies the $\mathcal{H}_2$ guaranteed cost (4.28).

Proof: We need to demonstrate that the conditions (4.29)-(4.31) satisfy the inequalities (4.26) for the close-loop system (4.13). Performing suitably the Schur Complement, we can rewrite (4.26) as

$$\begin{bmatrix} \mathcal{P}_i[n] & \bullet & \bullet \\ \tilde{\mathcal{A}}_{ij[n]} & \mathcal{P}_i[n+1]^{-1} & \bullet \\ \tilde{\mathcal{C}}_{ij[n]} & 0 & I \end{bmatrix} > 0 \tag{4.32}$$

Notice that, from (4.16) for $i \neq j[n]$ we have that $\tilde{\mathcal{A}}_{ij[n]} = \mathcal{A}_{ij[n]}$ and $\tilde{\mathcal{C}}_{ij[n]} = \mathcal{C}_{ij[n]}$ and, therefore, multiplying both sides of (4.33) for $\mathrm{diag}\{\mathcal{P}[n]^{-1}, I, I\}$ we obtain directly (4.30). Now, considering the case in which $i = j[n]$ and multiplying to the right of (4.33) by $\mathrm{diag}\{\mathcal{G}_i, I, I\}$ and to the left by its transpose, we obtain

$$\begin{bmatrix} \mathcal{G}_i'\mathcal{P}_i[n]\mathcal{G}_i & \bullet & \bullet \\ (\mathcal{A}_{ij} + \mathcal{B}_{ij}\mathcal{K}_i)\mathcal{G}_i & \mathcal{P}_i[n+1]^{-1} & \bullet \\ (\mathcal{C}_{ij} + \mathcal{D}_{ij}\mathcal{K}_i)\mathcal{G}_i & 0 & I \end{bmatrix} > 0 \tag{4.33}$$

Using the well known lower bound proposed in (OLIVEIRA; BERNUSSOU; GEROMEL, 1999)

$$\mathcal{G}_i'\mathcal{X}_i[n]^{-1}\mathcal{G}_i \geq \mathcal{G}_i + \mathcal{G}_i' - \mathcal{X}_i[n] \tag{4.34}$$

and take into account that $\mathcal{K}_i = \mathcal{Y}_i\mathcal{G}_i^{-1}$ we obtain (4.29). The last inequality (4.31) comes directly from the upper bound $\mathcal{H}_i'\mathcal{P}_i[0]\mathcal{H}_i < \mathcal{W}_i$. The proof is concluded. □

Notice that this theorem is expressed in terms of LMIs and, therefore, can be solved without any difficulty. The same remark can not be drawn on the cooperative control technique proposed in (SOUSA; GEROMEL; DEAECTO, 2015) since it is based on Lyapunov-Metzler inequalities that are nonconvex and therefore very difficult to solve.

Academical Example: In order to compare our methodology with respect to the one proposed in (SOUSA; GEROMEL; DEAECTO, 2015), we have solved the conditions of Theorem 4.2 for the same practical application example presented in (SOUSA; GEROMEL; DEAECTO, 2015). It consists on the control of two decoupled inverted pendulums with masses $m_1 = 2$ [kg], $m_2 = 4$ [kg] and equal lengths $\ell_1 = \ell_2 = 1$ [m], mounted on two cars with equal masses $M_1 = M_2 = 10$ [kg] that are subject to horizontal forces with intensities $f_i, i \in \{1, 2\}$. It is adopted $g = 9.8$ [m/s^2]. The model is given by

$$\begin{aligned}(M_i + m_i)\ddot{r}_i - m_i\ell_i\ddot{\theta}_i &= f_i \\ \ddot{r}_i - \ell_i\ddot{\theta}_i + g\theta_i &= 0\end{aligned} \tag{4.35}$$

The input variables are $u_i = f_i$ and the controlled output variable is $z_i = [r_i \;\; \theta_i \;\; d_i u_i]'$.The force intensity has the weights $d_1 = d_2 = 0.5$. Matrices $H_1 = [0 \;\; 0 \;\; \pi/3 \; 0]'$ and $H_2 = [0 \;\; 0 \;\; -\pi/4 \; 0]'$ define the initial condition of each pendulum in radians with respect to the vertical. The sampling period is $h = 200$ [ms]. Solving the conditions of Theorem 4.2 for $\kappa = 4$, we have obtained an $\mathcal{H}_2$ guaranteed cost of $J_2(\sigma) < 1.5212 \times 10^4$, correspondent to $\mathfrak{C}_6(4) = [1 \;\; 2 \;\; 1 \;\; 2]$ and the following state feedback gains

$$\begin{aligned}L_1 &= \begin{bmatrix}0.4517 & 1.9632 & -159.5755 & -46.8147\end{bmatrix} \\ L_2 &= \begin{bmatrix}0.4083 & 1.8744 & -179.4035 & -48.9317\end{bmatrix}\end{aligned}$$

with $K_1 \approx K_2 \approx 0$. For this particular example, we have obtained almost same guaranteed performance of reference (SOUSA; GEROMEL; DEAECTO, 2015) indicating that our methodology is easier to solve but not more conservative than the one based on Lyapunov-Metzler inequalities.

The next section validates experimentally the theory by means the cooperative control of an inverted pendulum and an active suspension.

4.2 Experimental Results

In this section, the $\mathcal{H}_2$ cooperative control strategy proposed in Theorem 4.2 is implemented for controlling jointly the inverted pendulum (QUANSER, 2012b) and the active suspension (QUANSER, 2012a), whose models have been presented in the previous chapter. The design must be carried out cooperatively sharing the same communication channel, that is, while one of the plants receives the updated control signal, the other keeps the signal previously received.

Figure 4.1 presents a photo of the experimental arrangement in the laboratory. It can be seen the active suspension to the left, the data acquisition board with the actuator in the middle and the pendulum to the right. The inverted pendulum presented in Chapter 4 presents the state space vector $x_1 = [x_c \; \theta \; \dot{x}_c \; \dot{\theta}]'$ and the control input $u_1 = V_{m1}$ and its mathematical model is given in (3.8) with matrices presented in (3.30). The state space representation of the active suspension is given in (3.31) with matrices provided in (3.33). Its mathematical model has been defined for the state vector $x_2 = [(z_s - z_{us}) \; \dot{z}_s \; (z_{us} - z_r) \; \dot{z_{us}}]'$ and the control effort $u_2 = F_{c2}$. The simulation and numerical routines have been performed on a computer with Windows 10 Pro using MATLAB R2018b 64-bit software with the help of the LMILab toolbox and Simulink. The numerical routine of Theorem 4.2 is available in the appendix of this thesis.

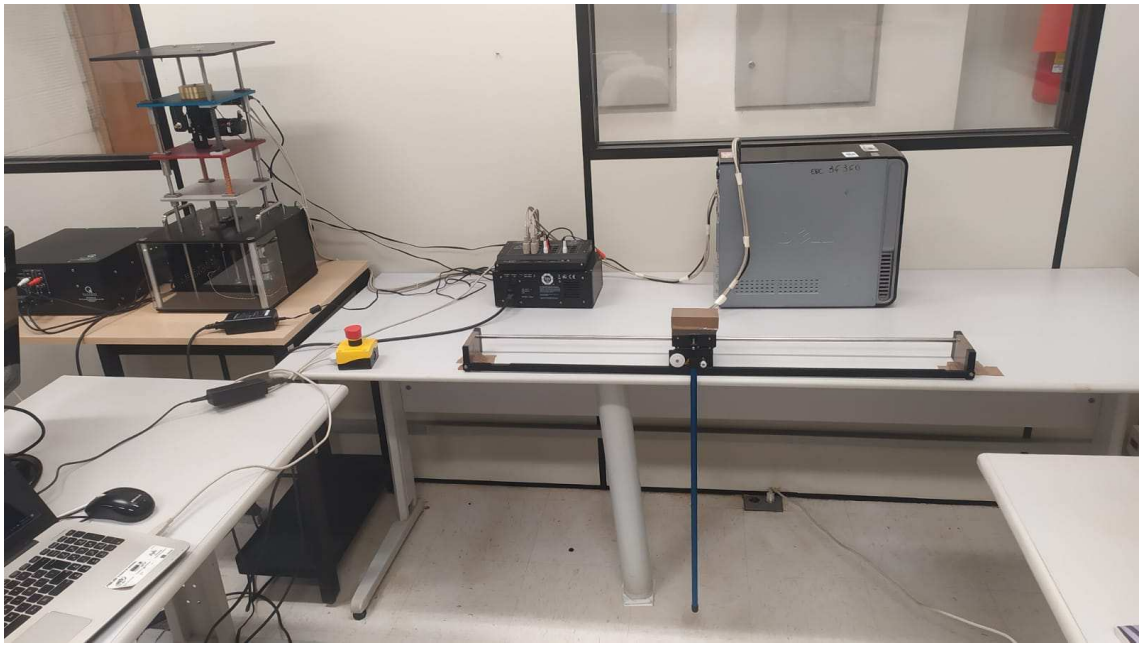

Figure 4.1: Real system mounted on the laboratory

4.2.1 $\mathcal{H}_2$ Control

For the $\mathcal{H}_2$ cooperative control, the system (4.1) is defined with the matrices already provided in Chapter 4 where the pendulum is identified as the first plant with $H_1 = x_0 = [0 \quad -\pi/18 \quad 0 \quad 0]'$ and the active suspension as the second plant. Let us consider that both plants evolve from the rest and that they have been discretized with a sampling period of $h = 10$ [ms]. We have solved the conditions of Theorem 4.2 for several values of $\kappa \in \{2, 3, 4, 5, 6, 7\}$ obtaining the guaranteed costs provided in the Table 4.1 as well the optimal combination $\mathfrak{C}_\ell(\kappa)^*$.

Tests for different κ		
κ	Guaranteed cost	Optimal $\mathfrak{C}_\ell(\kappa)^*$
2	4.1164	[1 2]
3	4.1212	[1 2 2]
4	**4.1164**	**[1 2 1 2]**
5	4.1196	[1 2 1 2 2]
6	4.1164	[1 2 2 1 2 2]
7	4.1189	[1 2 1 2 1 2 2]

Table 4.1: Determination of the best κ for the experimental test

Hence, for $\kappa = 4$ we have obtained the state-feedback gains

$$L_1 = \begin{bmatrix} 38.8004 & -108.1505 & 34.2317 & -22.5134 \end{bmatrix}$$

$$L_2 = \begin{bmatrix} 230.5545 & -81.6769 & 88.3745 & -0.0034 \end{bmatrix}$$

with $K_1 = K_2 \approx 0$ as well as the Lyapunov matrices

$$P_{10} = \begin{bmatrix} 58.6598 & -45.5979 & 19.7390 & -9.6379 & -6.2328e{-}9 \\ -45.5979 & 59.9692 & -22.9206 & 12.5981 & 1.0183e{-}7 \\ 19.739 & -22.9206 & 9.1359 & -4.8260 & -1.3390e{-}8 \\ -9.6379 & 12.5981 & -4.8260 & 2.6470 & 1.2648e{-}9 \\ -6.2328e{-}9 & 1.0183e{-}7 & -1.3390e{-}8 & 1.2648e{-}9 & 2.3954{-}9 \end{bmatrix}$$

$$P_{11} = \begin{bmatrix} 58.9528 & -49.0841 & 20.8516 & -10.3640 & -0.0301 \\ -49.0841 & 69.3661 & -25.9196 & 14.5554 & 0.0812 \\ 20.8516 & -25.9196 & 10.0930 & -5.4506 & -0.0259 \\ -10.3640 & 14.5554 & -5.4506 & 3.0547 & 0.0169 \\ -0.0301 & 0.0812 & -0.0259 & 0.0169 & 0.0007 \end{bmatrix}$$

$$P_{12} = \begin{bmatrix} 58.6598 & -45.5980 & 19.7390 & -9.6379 & -3.2601e-9 \\ -45.5979 & 59.9693 & -22.9207 & 12.5982 & 8.6059e-7 \\ 19.7390 & -22.9206 & 9.1359 & -4.8260 & -2.7069e-8 \\ -9.6379 & 12.5982 & -4.8260 & 2.6470 & 11.7090e-9 \\ -3.2601e-9 & 8.6059e-7 & -2.7069e-7 & 1.7090e-7 & 7.1063e-9 \end{bmatrix}$$

$$P_{13} = \begin{bmatrix} 59.9528 & -49.0841 & 20.8515 & -10.3640 & -0.0301 \\ -49.5980 & 69.3659 & -25.9195 & 14.5553 & 0.0812 \\ 20.8515 & -25.9195 & 10.0929 & -5.4506 & -0.0259 \\ -10.3640 & 14.5553 & -5.4506 & 3.0547 & 0.0169 \\ -0.0301 & 0.0812 & -0.0259 & 0.0169 & 0.0007 \end{bmatrix}$$

for the first subsystem, and

$$P_{20} = \begin{bmatrix} 1.7760 & -0.0015 & 1.8741 & -0.0005 & -2.7905e-5 \\ -0.0015 & 0.0088 & 0.0058 & 0.0009 & 2.3785e-5 \\ 1.8741 & 0.0058 & 2.2967 & 0.0003 & 5.0450e-6 \\ -0.005 & 0.0009 & 0.0003 & 0.0002 & 1.8201e-6 \\ -2.7905e-5 & 2.3785e-5 & 5.0450e-6 & 1.8201e-6 & 2.4236e-7 \end{bmatrix}$$

$$P_{21} = \begin{bmatrix} 1.7760 & -0.0020 & 1.8776 & -0.0002 & 1.3304e-6 \\ -0.0020 & 0.0066 & 0.0058 & 0.0007 & 4.82615e-7 \\ 1.8776 & 0.0058 & 2.2986 & 0.0002 & 6.7122e-7 \\ -0.0002 & 0.0007 & 0.0002 & 0.0002 & 1.8201e-6 \\ 1.3304e-6 & 4.82615e-7 & 6.7122e-7 & 1.8201e-6 & 2.6736e-7 \end{bmatrix}$$

$$P_{22} = \begin{bmatrix} 1.7760 & -0.0020 & 1.8776 & -0.0002 & 2.5429e-5 \\ -0.0012 & 0.0066 & 0.0058 & 0.0007 & 3.9168e-5 \\ 1.8743 & 0.0058 & 2.2986 & 0.0002 & 1.7453e-5 \\ -0.0004 & 0.0007 & 0.0002 & 0.0002 & 2.8100e-6 \\ 2.5429e-5 & 3.9168e-5 & 1.7453e-5 & 2.8100e-6 & 3.7517e-7 \end{bmatrix}$$

$$P_{23} = \begin{bmatrix} 1.7760 & -0.0025 & 1.8789 & -0.0002 & 4.1465e-6 \\ -0.0025 & 0.0068 & 0.0062 & 0.0007 & 1.2699e-6 \\ 1.8789 & 0.0062 & 2.2994 & 0.0002 & 2.4122e-6 \\ -0.0002 & 0.0007 & 0.0002 & 0.0002 & 5.2975e-8 \\ 4.1465e-6 & 1.2699e-6 & 2.4122e-6 & 5.2975e-8 & 6.4567e-7 \end{bmatrix}$$

for the second subsystem. which are essential for switching function implementation.

This control strategy has been implemented in the laboratory for the pendulum evolving from $x_0 = H_1$ and the suspension perturbed by the external input $w(t) = \dot{z}_r(t)$ where z_r is the road profile represented by a square wave signal with amplitude 0.02 [m] and period of 4 [s] with 50% of pulse width. This signal has been differentiated by means of a filter with transfer function $2.5e5s/(s^2 + 1e3s + 2.5e5)$ in order to obtain the disturbance $w = \dot{z}_r$. We have repeated the experimental tests 25 times. Figure 4.2 presents the state trajectories of the pendulum at the top and the active suspension at the bottom. In this figure, the shaded area represents one standard deviation of the mean, the dashed line corresponds to one of the measures among the 25 available ones and the continuous line the correspondent numerical simulation.

Figure 4.3 presents the control effort $u_i[n]$ and the switching rule (coordinator $\sigma[n]$) related to the same experimental test previously chosen, for $i = 1, 2$. Notice in the zoom made in the graph the cooperative nature of the control efforts, that is, when $u_1[n]$ is updated $u_2[n]$ remains constant and *vice-versa*.

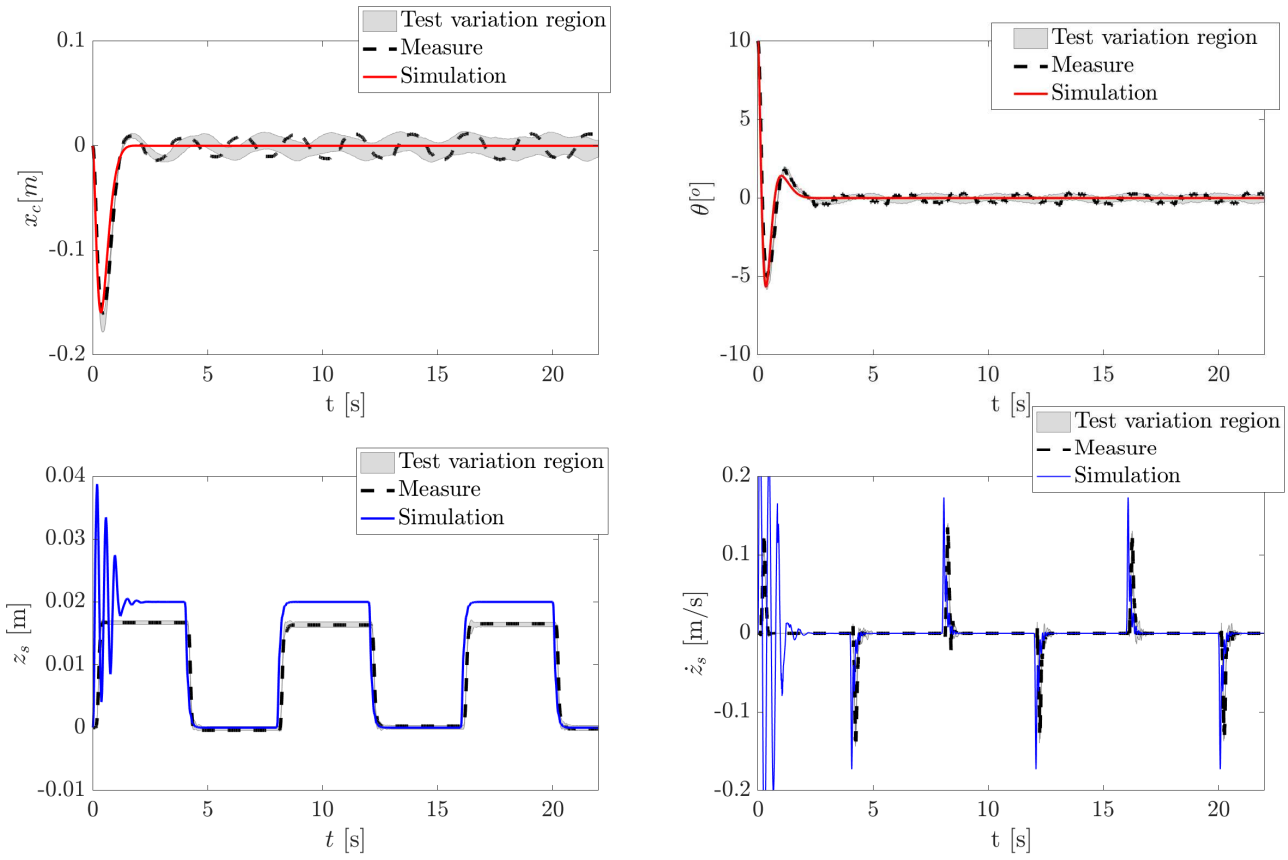

Figure 4.2: State trajectories of the pendulum at the top and the suspension at the bottom

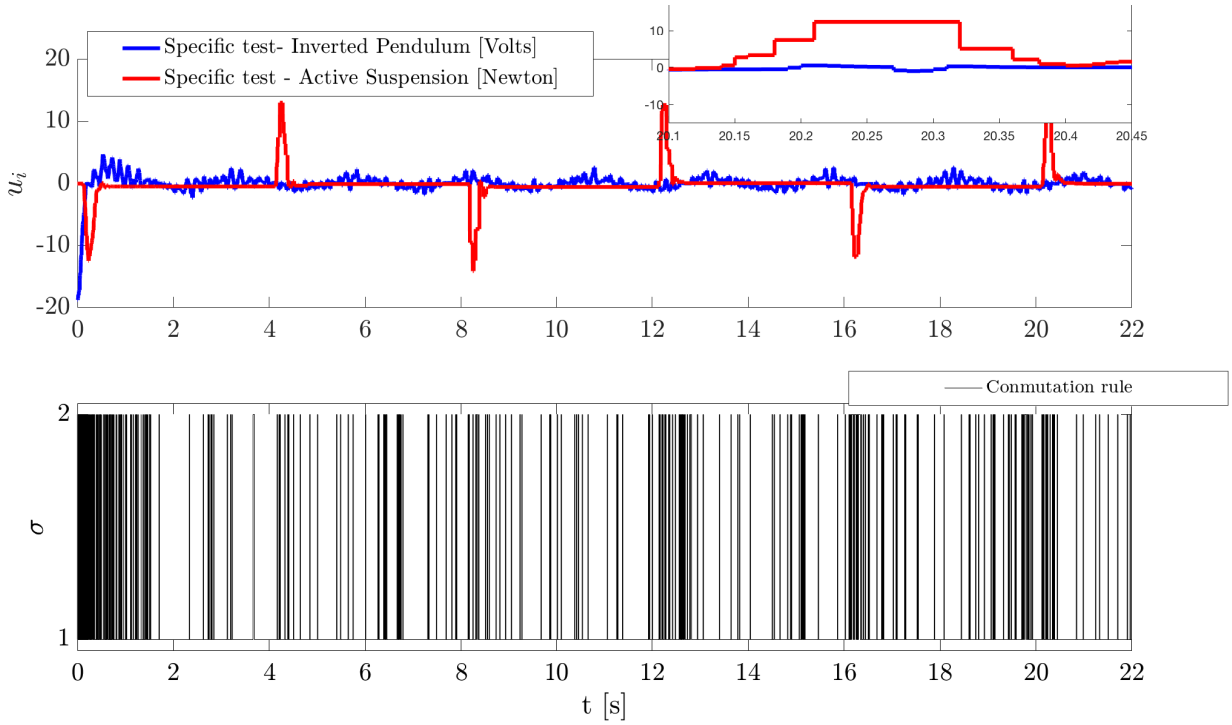

Figure 4.3: Cooperative control law and the correspondent switching function

Analysing and comparing the responses, we can conclude that the cooperative control technique is very efficient in stabilizing both plants. Moreover, the measures were very near the simulated data. Notice that the difference observed in the displacement of the chassis z_s is due to the Coulomb friction which has not been considered in the model. It is important to emphasize the robustness of the control strategy despite several phenomena and uncertainties that have been ignored during system modeling.

4.3 Final Considerations

In this chapter, we have presented the main results of this thesis. More specifically, an $\mathcal{H}_2$ cooperative control technique has been elaborated based on a time-varying periodic Lyapunov function, which is easier, but not more conservative, than other control techniques available in the literature. These conditions have been experimentally validated in the cooperative control of the inverted pendulum and the active suspension presented in the previous chapter.The obtained measures made clear the validity of the theory and the efficiency of the control methodology.

Chapter 5

Conclusion

In this thesis, we have proposed a novel cooperative control technique for LTI systems that share the same communication network with limited bandwidth. More specifically, the control law must respect the bandwidth limitation of the communication channel as well as operate in a cooperative way, sharing the resources adequately among the available plants. A coordinator, represented by the switching function, is responsible for selecting at each sampling instant which plant must receive the updated control signal, while the others keep the previous information. The switching rule has an essential role in the cooperative system to assure global asymptotic stability for all the plants as well as a good $\mathcal{H}_2$ guaranteed performance. This problem has already been treated in the literature, but by means of non-convex conditions expressed in terms of Lyapunov-Metzler inequalities, which are very difficult to solve, (SOUSA; GEROMEL; DEAECTO, 2015). Our main contribution in this sense is to provide alternative conditions expressed by LMIs and that can be solved without difficulty. These conditions are based on a time-varying periodic Lyapunov function and represents a generalization of the results from (DAIHA et al., 2017) that treats analysis and control design of switched linear systems, exclusively, without considering networked control nor cooperative control. The proposed control methodology bas been applied in an inverted pendulum and an active suspension, both from Quanser® company. Our experimental results have clearly shown the efficiency and the accuracy of the proposed technique.

Appendix

Codes

5.0.1 Theorem 2.2

```
function [Pio,Jop,Po] = Example_LyapunoMetzler(A,C,Periodo,ci,Precision)
% El sistema descrito por A, C debe ser en tiempo continuo.


%Normal matrixes
Ac{1}=A{1};
Ac{2}=A{2};
T=Periodo;
N = size(Ac,2);
nx=size(Ac{1},1);
%Discretisacion
for k=1:N
    Ad{k}=expm(Ac{k}*T); %expm is matrix exponential..
    %exp just applies exp function to
    %every matrix entry
end
Cd{1}=C{1};
Cd{2}=C{2};
x0=ci; %vector columna
nz = size(Cd{1},1);
%Inicializamos este valor
Jop = inf;
%%%%%%%%%%%%%%%%%%%%%%%%%%%%%%%%%%%%%%%%%%%%%%%%%%%%%%%%%%%%%%%%%%%%%%%%%%%%%%%
%%%%%%%%%%%%%%%%%%%%%%%%%Problema%%%%%%%%%%%%%%%%%%%%%%%%%%%%%%%%%%%%%%%%%%%%%
%%%%%%%%%%%%%%%%%%%%%%%%%%%%%%%%%%%%%%%%%%%%%%%%%%%%%%%%%%%%%%%%%%%%%%%%%%%%%%%
ps = 0:Precision:1;
qs = 0:Precision:1;
for  i=1:length(ps)
    for  j=1:length(qs)
        % Resetea las LMI internas
        Pim=[ps(i) 1-qs(j) ;1-ps(i) qs(j)];
        [Ps,Js] = lyapunov_metzler(Ad,Cd,Pim,x0);
        if isempty(Ps)
            cost(i,j) = NaN;
        else
            cost(i,j)= Js;
            if Js<Jop
                Po = Ps;
                Jop = Js;
```

```
40                  Pio = Pim;
41              end
42          end
43      end
44  end
45  %mesh(qs,ps,cost)clc
46  %axis([200,400,200,400,300,1000])
47
48      function [Ps,Js] = lyapunov_metzler(Ad,Cd,Pim,x0)
49          nx = size(Ad{1},1);
50          N = size(Ad,2);
51
52          setlmis([]);
53          %Declaracion de variables
54          %===============
55          for i=1:N
56              P{i} = lmivar(1,[nx 1]);
57          end
58          W = lmivar(1,[nx 1]);
59          %===============
60          %Primer y segundo LMI
61          for i=1:N
62              ct = newlmi;
63              lmiterm([-ct,1,1,P{i}],1,1);
64              for j=1:N
65                  lmiterm([-ct,2,1,P{j}],Pim(j,i),Ad{i});
66                  lmiterm([-ct,2,2,P{j}],Pim(j,i),1);
67              end
68              lmiterm([-ct,3,1,0],Cd{i});
69              lmiterm([-ct,3,3,0],1);
70          end
71
72          %Tercer y cuarta LMI
73          for i=1:N
74              ct = newlmi;
75              lmiterm([-ct,1,1,P{i}],1,1);
76          end
77          ct = newlmi;
78          for i = 1:N
79              lmiterm([ct,1,1,P{i}],1,1);
80          end
81          lmiterm([ct,1,1,W],-1,1);
82
83          lmisys = getlmis;
84          options = [1e-4,2000,1e9,1000,0];
85          np = decnbr(lmisys);
86          c = zeros(np,1);
87
88          for h=1:np
89              % defcx returns the values V1,...,Vk of these variables when the
90              % n-th decision variable is set to one and all others to zero.
91              [Wh] = defcx(lmisys,h,W);
92              %Definiendo la funcion objetivo de acuerdo a cada uno de las ...
                    variables de
93              %decision ( de P )
94              c(h) = x0'*Wh*x0;
95          end
```

```

        %Minimize linear objective under LMI constraints
        [copt,xopt] = mincx(lmisys,c,options);
        if (isempty(copt))
            Ps = [];
            Js = [];
        else
            %Devuelve el valor de P en base a xopt
            for i=1:N
                Ps{i} = dec2mat(lmisys,xopt,P{i});
            end
            Js = copt; % Norma ao quadrado
        end

    end
end
```

5.0.2 2.4.3 Example

```
function [Po,Jop,otimacom] = Example_tvLyapunov(A,C,ci,kappa,Period)
%El sistema A, C debe ser presentado en tiempo continuo.

T=Period;
N = size(A,2);
nx=size(A{1},1);
%Discretisacion
for k=1:N
    Ad{k}=expm(A{k}*T); %expm is matrix exponential..
                        %exp just applies exp function to
                        %every matrix entry
end
Cd{1}=C{1};
Cd{2}=C{2};
x0=ci;
nz = size(Cd{1},1);
%Inicializamos este valor
Jop = inf;
%Numero de elemetos a permutar
Item = N;
desired=kappa;
Kappa_T=zeros(desired-1,1);
Js_T=zeros(desired-1,Item^desired);
J_LMI=zeros(desired-1,1);
J_argmin=zeros(desired-1,1);
for Kap=2:desired

%%%%%%%%%%%%%%%%%%%%%%%%%%%%%%%%%%%%%%%%%%%%%%%%%%%%%%%%%%%%%%%%%%%%%%%%%%%%%%%
%%%%%%%%%%%%%%%%%%%%%%%%%%%%LMI%%%%%%%%%%%%%%%%%%%%%%%%%%%%%%%%%%%%%%%%%%%%%%%%
%%%%%%%%%%%%%%%%%%%%%%%%%%%%%%%%%%%%%%%%%%%%%%%%%%%%%%%%%%%%%%%%%%%%%%%%%%%%%%%
%L matriz que tiene las permutaciones
L = permutations(Item,Kap);
for i=1:Item^Kap
    % Resetea las LMI internas
    [Ps,Js] = lmi_condition(Ad,Cd,x0,L(i,:));
```

```
    if isempty(Ps)
        cost(i) = NaN;
    else
        cost(i)= Js;
        Js_T(Kap-1,i)=Js;
        if Js<Jop
            Po = Ps;
            Po_T{Kap-1,:}=Po;
            Jop = Js;
            J_LMI(Kap-1,1)=Jop;
            otimacom = L(i,:);
            Otimacom_T{Kap-1,:}=otimacom;
        end
    end
end
%Restart the Jop;
Jop = inf;
Kappa_T=[2:desired]';
end

%mesh(qs,ps,cost)
%axis([200,400,200,400,300,1000])

%%%%%%%%%%%%%%%%%%%%%%%%%%%%%%%%%%%%%%%%%%%%%%%%%%%%%%%%%%%%%%%%%%%%%%%%%%%%%%%
%%%%%%%%%%%%%%%%%%%%%%%%%ONLINE_SWITCHING%%%%%%%%%%%%%%%%%%%%%%%%%%%%%%%%%%%%%
%%%%%%%%%%%%%%%%%%%%%%%%%%%%%%%%%%%%%%%%%%%%%%%%%%%%%%%%%%%%%%%%%%%%%%%%%%%%%%%

nmax=fix(10/T);
x0=[-1 1 1]';
sig=zeros(1,nmax-1);
x=zeros(nx,nmax);
z=zeros(nz,nmax-1);
x(:,1)=x0;

%%
for Kap=2:desired
    Po=Po_T{Kap-1,:};
for n=2:nmax
    for i=1:N
        v(i)=x(:,n-1)'*(Ad{i}'*Po{mod(n-1,Kap)+1}*Ad{i}+ Cd{i}'*Cd{i})*x(:,n-1);
    end
    [vmin,idx] = min(v);
    x(:,n)=Ad{idx}*x(:,n-1  );

    sig(n-1)=idx;
    z(:,n-1) = Cd{idx}*x(:,n-1);
end
actual_cost = trace(z'*z);
J_argmin(Kap-1,1)=actual_cost;
end

% Para graficar

subplot(2,1,1)
axis=subplot(2,1,1)
stairs(0:nmax-1,x(1,:),'LineWidth',2,'Marker','o','MarkerFaceColor','c')
hold on
```

```
stairs(0:nmax-1,x(2,:),'LineWidth',2,'Marker','o','MarkerFaceColor','r')
hold on
stairs(0:nmax-1,x(3,:),'LineWidth',1.5,'Marker','o','MarkerFaceColor','g')
set(gca,'FontSize',20)
legend({'$x_{1}$','$x_{2}$','$x_{3}$'},'FontSize',14,'Interpreter','latex')
ylabel('$x(n)$','FontSize',20,'Interpreter','latex')
set(axis,'FontWeight','bold','TickLabelInterpreter','latex');
%axis([0 100 -2.5 1.2])



subplot(2,1,2)
axis=subplot(2,1,2)
stairs(0:nmax-2,sig,'LineWidth',1,'MarkerFaceColor','b')
hold on
plot(0:nmax-2,sig,'or','LineWidth',2)
set(gca,'FontSize',18)
ylabel('$\sigma(n)$','FontSize',20,'Interpreter','latex')
xlabel('$n$','FontSize',20,'Interpreter','latex')
set(axis,'FontWeight','bold','TickLabelInterpreter','latex');
ylim([0.8 2.2])
%axis([0 100 0.8 2.2])

%%

%Conmutacion
%Tiempo de simulacion
Time=10
%Puntos de la simulacion
nmax=ceil(Time/T);

sig=zeros(1,nmax-1);
x=zeros(nx,nmax);
z=zeros(nz,nmax-1);

%Inicializando
x(:,1)=x0;

%%%%%%%%%%%%%
%Permutation%
%%%%%%%%%%%%%
for Kap=2:desired
    L=Otimacom_T{Kap-1,:};
%
nl = size(L,2);
%Contains all the subindexes
Permut=[];
for n=1:ceil(nmax/nl)
   Permut=[Permut,L];
end

for n=2:nmax
    idx=Permut(1,n-1);
    x(:,n)=Ad{idx}*x(:,n-1);
    z(:,n-1)= Cd{idx}*x(:,n-1);
end
actual_cost_periodic = trace(z'*z)
```

```
J_periodic(Kap-1,1)=actual_cost_periodic;
end

%%%%%%%%%%%%%%%%%%%%%%%%%%%%%%%%%%%%%%%%%%%%%%%%%%%%%%%%%%%%%%%%
%TABLE=table(Kappa_T,Js_T,J_LMI,Otimacom_T,J_argmin,J_periodic);%
%%%%%%%%%%%%%%%%%%%%%%%%%%%%%%%%%%%%%%%%%%%%%%%%%%%%%%%%%%%%%%%%%

%%%%%%%%%%%%%%%%%%%%%%%%%%%%%%%%%%%%%%%%%%%%%%%%
TABLE=table(Kappa_T,J_LMI,J_periodic,J_argmin);%
%%%%%%%%%%%%%%%%%%%%%%%%%%%%%%%%%%%%%%%%%%%%%%%%


%%%%%%%%%%%%%%%%%%%%%%%%%%%%%%%%%%%%%%%%%%%%%%%%%%%%%%%%%%%%%%%%%%%%%%%%%%
DEFINICION DE FUNCIONES%%%%%%%%%%%%%%%%%%%%%%%%%%%%
%%%%%%%%%%%%%%%%%%%%%%%%%%%%%%%%%%%%%%%%%%%%%%%%%%%%%%%%%%%%%%%%%%%%%%%%%%

function [Ps0,Js] = lmi_condition(Ad,Cd,x0,L)
%Cuantas incognitas wtiene nuestra variable
nx = size(Ad{1},1);
%Cuantas LMI vamos ter
N = size(Ad,2);

setlmis([]);
Kap = length(L);
for i=1:Kap
    P{i} = lmivar(1,[nx 1]);
end

P{Kap+1} = P{1};

for i=1:Kap
    ct = newlmi;
    lmiterm([ct,1,1,P{i+1}],Ad{L(1,i)}',Ad{L(1,i)});
    lmiterm([ct,1,1,0],Cd{L(1,i)}'*Cd{L(1,i)});
    lmiterm([ct,1,1,P{i}],-1,1);
end

%Third LMI

for i=1:Kap
    ct = newlmi;
    lmiterm([-ct,1,1,P{i}],1,1);
end

lmisys = getlmis;
options = [1e-6,2000,1e9,10000,1];
np = decnbr(lmisys);
c = zeros(np,1);

for h=1:np
    % defcx returns the values V1,...,Vk of these variables when the
    % n-th decision variable is set to one and all others to zero.
    [Psopt] = defcx(lmisys,h,P{Kap+1});
    %Defining la funcion objetivo de acuerdo a cada uno de las variables de
    %decision ( de P )
    c(h) = x0'*Psopt*x0;
end
```

```
207
208 %Minimize linear objective under LMI constraints
209 [copt,xopt] = mincx(lmisys,c,options);
210 if (isempty(copt))
211     Ps0 = [];
212     Js = [];
213 else
214     %Devuelve el valor de P en base a xopt
215     for n=1:Kap
216         Ps0{n}= dec2mat(lmisys,xopt,P{n});
217     end
218     Ps0{n+1} = Ps0{1};
219     Js = copt; % Norma ao quadrado
220 end
221
222 end
223
224
225 %Crea todas las permutaciones
226 function[L] = permutations(N,Kappa)
227 %Lista de los sistemas a permutar
228 %Num={1,2,3,...N}
229 Num=1:N;
230 %Matriz con todas las permutaciones
231 L = zeros(N^Kappa,1);
232 %Posicion en la lista
233 c = 1;
234 for a=1:Kappa
235     for b=1:N^Kappa
236         conj=(N^Kappa)/(N^a);
237         if (c-1) == N
238             c=1;
239         end
240         if (mod(b,conj)) ~= 0
241             L(b,a) = Num(c);
242         else
243             L(b,a) = Num(c);
244             c=c+1;
245         end
246     end
247     c=1;
248 end
249 end
250 %Lyapunov
251 %H2
252 %Conditions for exponential stability, given a discrete linear system.
253 end
```

5.0.3 Proposed Methodology

```
1 function [Po,Ka,Jopt,otimacom] = ...
     ProposedMethodology(An,Bn,Cn,Dn,Hn,Periodo,Kappa)
2 %El sistema An, Bn, Cn, Dn debe ser presentado en tiempo continuo.
3 T=Periodo;
```

```
4
5  %%%%%%%%%%%%%%%%%%%%%%%%%%%%
6  %Para el carro y el pendulo%
7  %%%%%%%%%%%%%%%%%%%%%%%%%%%%
8
9  %Variables d estado : [Desp  Angle dot(Desp) dot(Angle)]
10
11 A{1}=An{1};
12 B{1}=Bn{1};
13 %Aca tienes que empezar a hacer la ponderacion
14 C{1} = Cn{1};
15 D{1}= Dn{1};
16 H{1}=Hn{1};%Vector columna
17
18 %%%%%%%%%%%%%%%%%%%%
19 %Para la suspension%
20 %%%%%%%%%%%%%%%%%%%%
21 %Set the model parameters of the Active Suspension.
22 %This section sets the A,B,C and D matrices for the Active Suspension model.
23
24 A{2} = An{2};
25 B{2} = Bn{2};
26 C{2} = Cn{2};
27 D{2} = Dn{2};
28 H{2}=Hn{2};
29
30 %Extrayendo numero de subsistemas
31 N = size(A,2);
32 %Discretizing
33 for k=1:N
34     [Ad{k}, Bd{k}, Cd{k}, Dd{k}] =  c2discrete(A{k}, B{k}, C{k}, D{k}, T);
35 end
36
37 % Augmented system
38
39 nx = size(Ad{1},1);
40 nu = size(Bd{1},2);
41 nw = size(H{1},2);
42
43
44 for i = 1:N
45     for j=1:N
46         if i==j
47             Aa{i,j}=[Ad{i} 0*Bd{i}; zeros(nu,nx) 0*eye(nu)];
48             Ba{i,j}=[Bd{i};eye(nu)];
49             Ca{i,j}=[Cd{i} 0*Dd{i}];
50             Da{i,j}=[Dd{i}];
51         else
52             Aa{i,j}=[Ad{i} Bd{i}; zeros(nu,nx) eye(nu)];
53             Ba{i,j}=[0*Bd{i};0*eye(nu)];
54             Ca{i,j}=[Cd{i} Dd{i}];
55             Da{i,j}=[0*Dd{i}];
56         end
57     end
58     Ha{i} = [H{i};zeros(nu,nw)];
59 end
60
```

```
%Inicializamos este valor
Jop = inf;
%Numero de elemetos a permutar
Item = N;
%Desidered = Kappa (Horizont)
%%%%%%%%%%%
Kap = Kappa;%
%%%%%%%%%%%%%%%%%%%%%%%%%%%%%%%%%%%%%%%%%%%%%%%%%%%%%%%%%%%%%%%%%%%%%%%%%%%%%%%
%%%%%%%%%%%%%%%%%%%%%%%%%%%%%LMI%%%%%%%%%%%%%%%%%%%%%%%%%%%%%%%%%%%%%%%%%%%%%%
%%%%%%%%%%%%%%%%%%%%%%%%%%%%%%%%%%%%%%%%%%%%%%%%%%%%%%%%%%%%%%%%%%%%%%%%%%%%%%%
L = permutations(Item,Kap);
Jopt = inf;

for i=1:size(L,1)
    % Resetea las LMI internas
    [Gs,Ys,Xs,Js] = lmi_condition(Aa,Ba,Ha,Ca,Da,L(i,:));
    if Js<Jopt
        %THIS STORES ALL THE VALUES!!! ( AFTER THE SIMULATION YOU CAN
        %CHEACK THE RESULTS WITH THE MATRIX 'COST'. is going to have
        %N^desired elements, which correspond to the cost for each combination
        Jopt = Js;
        Xo = Xs;
        Go = Gs;
        Yo = Ys;
        otimacom = L(i,:);
    end
end

Jopt
otimacom

for i=1:N
    for n=1:Kap
        Po{i,n}=Xo{i,n}^(-1);
    end
    Ka{i}=Yo{i}/Go{i};
end

for j=1:N
    for i = 1:N
        Aat{i,j} = Aa{i,j}+Ba{i,j}*Ka{i};
        Cat{i,j} = Ca{i,j}+Da{i,j}*Ka{i};
    end
end


%%
%%%%%%%%%%%%%%%%%%%%%%%%%%%%%%%%%%%%%%%%%%%%%%%%%%%%%%%%%%%%%%%%%%%%%%%%%%%%%%%
%%%%%%%%%%%%%%%%%%%%%%%LMI DECLARATION%%%%%%%%%%%%%%%%%%%%%%%%%%%%%%%%%%%%%%%%
%%%%%%%%%%%%%%%%%%%%%%%%%%%%%%%%%%%%%%%%%%%%%%%%%%%%%%%%%%%%%%%%%%%%%%%%%%%%%%%
    function[Gs,Ys,Xs,Js] = lmi_condition(Aa,Ba,Ha,Ca,Da,idx)
        %Cuantas incognitas wtiene nuestra variable
        nx = size(Aa{1},1);
        nu = size(Ba{1},2);
        nw = size(Ha{1},2);

        %Cuantas LMI vamos ter
```

```
118         N = size(Aa,2);
119         Kap = length(idx);
120
121         setlmis([]);
122         %%%%%%%%%%%%%%%%%%%%%%%%%
123         %%Variables definition%%%
124         %%%%%%%%%%%%%%%%%%%%%%%%%
125         for i=1:N
126             %We are adding one more (nx +1) because we are going to have ...
                    augmented matrices
127             %later
128             W{i} = lmivar(1,[nw,1]);
129             G{i} = lmivar(2,[nx,nx]);
130             Y{i} = lmivar(2,[nu,nx]);
131             for n=1:Kap
132                 X{i,n} = lmivar(1,[nx 1]);
133             end
134             X{i,Kap+1} = X{i,1};
135         end
136         R = lmivar(1,[nw,1]);
137         %%%%%%%%%%%%%%%
138         %FIRST LMIS%
139         %%%%%%%%%%%%%%%
140         for i = 1:N
141             for n = 1:Kap
142                 if idx(n) == i
143                     ct = newlmi;
144                     lmiterm([-ct,1,1,G{i}],1,1,'s');
145                     lmiterm([-ct,1,1,X{i,n}],-1,1);
146                     lmiterm([-ct,2,1,G{i}],Aa{i,idx(n)},1);
147                     lmiterm([-ct,2,1,Y{i}],Ba{i,idx(n)},1);
148                     lmiterm([-ct,2,2,X{i,n+1}],1,1);
149                     lmiterm([-ct,3,1,G{i}],Ca{i,idx(n)},1);
150                     lmiterm([-ct,3,1,Y{i}],Da{i,idx(n)},1);
151                     lmiterm([-ct,3,3,0],1);
152                 else
153                     ct = newlmi;
154                     lmiterm([-ct,1,1,X{i,n}],1,1);
155                     lmiterm([-ct,2,1,X{i,n}],Aa{i,idx(n)},1);
156                     lmiterm([-ct,2,2,X{i,n+1}],1,1);
157                     lmiterm([-ct,3,1,X{i,n}],Ca{i,idx(n)},1);
158                     lmiterm([-ct,3,3,0],1);
159                 end
160             end
161             ct = newlmi;
162             lmiterm([-ct,1,1,W{i}],1,1);
163             lmiterm([-ct,2,1,0],Ha{i});
164             lmiterm([-ct,2,2,X{i,1}],1,1);
165         end
166         ct = newlmi;
167         for i = 1:N
168             lmiterm([ct,1,1,W{i}],1,1);
169         end
170         lmiterm([ct,1,1,R],-1,1);
171
172         lmisys = getlmis;
173         options = [1e-6,200,1e9,10000,0];
```

```
174
175         np = decnbr(lmisys);
176         c = zeros(np,1);
177
178         for i = 1:np
179             Ri = defcx(lmisys,i,R);
180             c(i) = trace(Ri);
181         end
182
183         [copt,xopt] = mincx(lmisys,c,options);
184         if (isempty(copt))
185             Xs = NaN;
186             Js = NaN;
187             Gs = NaN;
188             Ys = NaN;
189             return
190         else
191             Js = copt;
192             for i = 1:N
193                 for n = 1:Kap
194                     Xs{i,n}= dec2mat(lmisys,xopt,X{i,n});
195                 end
196                 Gs{i}= dec2mat(lmisys,xopt,G{i});
197                 Ys{i}= dec2mat(lmisys,xopt,Y{i});
198                 X{i,n+1} = X{i,1};
199             end
200         end
201     end
202 %Todas las permutaciones se crearon en otro entorno
203     function[L] = permutations(N,Kappa)
204         %Lista de los sistemas a permutar
205         %Num={1,2,3,...N}
206         Num=1:N;
207         %Matriz con todas las permutaciones
208         L = zeros(N^Kappa,1);
209         %Posicion en la lista
210         c = 1;
211         for a=1:Kappa
212             for b=1:N^Kappa
213                 conj=(N^Kappa)/(N^a);
214                 if (c-1) == N
215                     c=1;
216                 end
217                 if (mod(b,conj)) ≠ 0
218                     L(b,a) = Num(c);
219                 else
220                     L(b,a) = Num(c);
221                     c=c+1;
222                 end
223             end
224             c=1;
225         end
226     end
227     function [Ad, Bd, Cd, Dd] = c2discrete(A, B, C, D, T)
228         %Discrete-time model
229         eps = 1e-8;
230         n = size(A,1);
```

```
231         m = size(B,2);
232         p = size(C,1);
233 
234         Aa = [A, B; zeros(m,n), zeros(m)];
235         G = [C,D];
236         M = expm(Aa*T);
237         Ad = M(1:n,1:n);
238         Bd = M(1:n,n+1:n+m);
239 
240         F = @(x) (G * expm(Aa*x))'*(G * expm(Aa*x));
241         %Use accumulator matrix, if given
242         Qd = quadv(F,0,T,eps);
243 
244         %Using SVD to decompose the matrix
245         [Q,S] = svd(Qd);
246         G = sqrt(S(1:n+m,1:n+m))*Q(:,1:n+m)';
247         Cd = G(:,1:n);
248         Dd = G(:,n+1:n+m);
249     end
250 
251 end
```

Bibliography

BOYD, S.; GHAOUI, L. E.; FERON, E.; BALAKRISHNAN, V. *Linear matrix inequalities in system and control theory*. [S.l.]: Siam, 1994. v. 15.

CHEN, T.; FRANCIS, B. A. *Optimal sampled-data control systems*. [S.l.]: Springer Science & Business Media, 2012.

DAI, S.; LIN, H.; GEE, S. S. A switched system approach to scheduling of networked control systems with communication constraints. *Proc. of the IEEE Conference on Decision and Control*, p. 4991–4996, 2009.

DAIHA, H. R.; EGIDIO, L. N.; DEAECTO, G. S.; GEROMEL, J. C. $\mathcal{H}_\infty$ state feedback control design of discrete-time switched linear systems. In: *IEEE Conference on Decision and Control*. [S.l.: s.n.], 2017. p. 5882–5887.

DEAECTO, G. S.; GEROMEL, J. C. Stability and performance of discrete-time switched linear systems. *Systems & Control Letters*, v. 118, p. 1–7, 2018.

DECARLO, R. A.; BRANICKY, M. S.; PETTERSSON, S.; LENNARTSON, B. Perspectives and results on the stability and stabilizability of hybrid systems. *Proc. of the IEEE*, v. 88, p. 1069–1082, 2000.

DONKERS, M. C. F.; HETEL, L.; HEEMELS, W. P. M. H.; WOUW, N. van de; STEINBUCH, M. Stability analysis of networked control systems using a switched linear systems approach. *Hybrid Systems: Computation and Control–Lecture Notes in Computer Science*, v. 5459, p. 150–164, 2009.

FIACCHINI, M.; GIRARD, A.; JUNGERS, M. On the stabilizability of discrete-time switched linear systems: Novel conditions and comparisons. *IEEE Transactions on Automatic Control*, v. 61, p. 1181–1193, 2016.

FIACCHINI, M.; JUNGERS, M. Necessary and sufficient condition for stabilizability of discrete-time linear switched systems: A set-theory approach. *Automatica*, v. 50, p. 75–83, 2014.

GEROMEL, J. C.; COLANERI, P. Stability and stabilization of continuous-time switched linear systems. *SIAM Journal on Control and Optimization*, p. 1915–1930, 2006.

GEROMEL, J. C.; COLANERI, P. Stability and stabilization of discrete time switched systems. *International Journal of Control*, v. 79, p. 719–728, 2006.

GEROMEL, J. C.; COLANERI, P.; BOLZERN, P. Dynamic output feedback control of switched linear systems. *IEEE Transactions on Automatic Control*, v. 53, p. 720–733, 2008.

GEROMEL, J. C.; DEAECTO, G. S.; DAAFOUZ, J. Suboptimal switching control consistency analysis for switched linear systems. *IEEE Transactions on Automatic Control*, v. 58, p. 1857–1861, 2013.

GEROMEL, J. C.; KOROGUI, R. H. *Controle linear de sistemas dinâmicos: Teoria, ensaios práticos e exercícios*. [S.l.]: Editora Edgard Blucher, 2001.

HESPANHA, J. P.; MORSE, A. S. Switching between stabilizing controllers. *Automatica*, v. 38, p. 1905–1917, 2002.

HESPANHA, J. P.; NAGHSHTABRIZI, P.; XU, Y. A survey of recent results in networked control systems. *Proc. of the IEEE*, v. 95, p. 138–162, 2007.

KHALIL, H. K. Nonlinear systems, 3rd. *New Jewsey, Prentice Hall*, 2002.

LIBERZON, D. *Switching in Systems and Control*. [S.l.]: Springer Science & Business Media, 2013.

LUZ NETTO, J. L. *Controle cooperativo $\mathcal{H}_2$ e $\mathcal{H}_\infty$ via rede de comunicação: Teoria e implementação prática em pêndulos invertidos*. Dissertação (Mestrado) — School of Mechanical Engineering - UNICAMP, 2018.

MAZO, M.; TABUADA, P. On event-triggered and self-triggered control over sensor/actuator networks. *Proc. of the IEEE Conference on Decision and Control*, p. 435–440, 2008.

MENG, X.; CHEN, T. Event triggered robust filter design for discrete-time systems. *IET Control Theory & Applications*, v. 8, p. 104–113, 2014.

OLIVEIRA, M. C. D.; BERNUSSOU, J.; GEROMEL, J. C. A new discrete-time robust stability condition. *Systems & control letters*, v. 37, p. 261–265, 1999.

QUANSER. *Active suspension system: User manual*. 2012. Markham, Ontario, Canada: Quanser Corporation.

QUANSER. *IP02 Linear Inverted Pendulum and IP02 Linear Pendulum Gantry Experiments: User manual*. 2012. Markham, Ontario, Canada: Quanser Corporation.

SHORTEN, R.; WIRTH, F.; MASON, O.; WULFF, K.; KING, C. Stability criteria for switched and hybrid systems. *SIAM review*, v. 49, p. 545–592, 2007.

SLOTINE, J.-J. E.; LI, W. *Applied nonlinear control*. [S.l.]: Prentice hall Englewood Cliffs, NJ, 1991. v. 199.

SOUSA, T. T. de; GEROMEL, J. C.; DEAECTO, G. S. Switching control resource allocation in networked control systems. *Proc. of the IEEE Conference on Decision and Control*, p. 6862–6867, 2015.

SOUZA, M.; DEAECTO, G. S.; GEROMEL, J. C.; DAAFOUZ, J. Self-triggered linear quadratic networked control. *Optimal Control Applications and Methods*, v. 35, p. 524–538, 2014.

SUN, Z. *Switched linear systems: control and design*. [S.l.]: Springer Science & Business Media, 2006.

WANG, F.; LIU, D. *Networked Control Systems: Theory and Applications*. London, England: Springer-Verlag, 2008.